

Superconnections in AdS/QCD and the hadronic light-by-light contribution to the muon $g - 2$

Josef Leutgeb, Jonas Mager, and Anton Rebhan
*Institut für Theoretische Physik, Technische Universität Wien,
Wiedner Hauptstrasse 8-10, A-1040 Vienna, Austria*
(Dated: February 25, 2025)

In this paper, we consider hard-wall AdS/QCD models extended by a string-theory inspired Chern-Simons action in terms of a superconnection involving a bi-fundamental scalar field which corresponds to the open-string tachyon of brane-antibrane configurations and which is naturally identified with the holographic dual of the quark condensate in chiral symmetry breaking. This realizes both the axial and chiral anomalies of QCD with a Witten-Veneziano mechanism for the η' mass in addition to current quark masses, but somewhat differently than in the Katz-Schwartz AdS/QCD model used previously by us to evaluate pseudoscalar and axial vector transition form factors and their contribution to the HLBL piece of the muon $g - 2$. Compared to the Katz-Schwartz model, we obtain a significantly more realistic description of axial-vector mesons with regard to f_1 - f_1' mixing and equivalent photon rates. Moreover, predictions of the $f_1 \rightarrow e^+e^-$ branching ratios are found to be in line with a recent phenomenological study. However, pseudoscalar transition form factors compare less well with experiment; in particular the π^0 transition form factor turns out to be overestimated at moderate non-zero virtuality. For the combined HLBL contribution to the muon $g - 2$ from the towers of axial vector mesons and excited pseudoscalars we obtain, however, a result very close to that of the Katz-Schwartz model.

I. INTRODUCTION

The anomalous magnetic moment of the muon has been measured to date with a world-average error of 0.19 ppm [1, 2], corresponding to a standard deviation of 22×10^{-11} in $a_\mu = (g - 2)_\mu/2$, and this uncertainty is expected to be further reduced by about a factor of 2 with the final result of the current experiment at Fermilab by the Muon $g - 2$ Collaboration. The Standard Model prediction of a_μ is limited by uncertainties in the contribution from hadronic vacuum polarization (HVP), where data-driven and lattice calculations aim at per-mille accuracy to match the experimental precision, but currently deviate from each other beyond their respective error estimates [3]. Once this discrepancy is resolved, the uncertainty of the much smaller hadronic light-by-light (HLBL) scattering contribution will be again of comparable importance as it contributes an error of 19×10^{-11} according to the 2020 White Paper of the Muon $g - 2$ Theory Initiative [4]. This uncertainty is dominated by the effect of short-distance constraints (SDCs) [5–14] and axial vector contributions, for which errors of 10×10^{-11} and 6×10^{-11} , respectively, have been estimated in [4], corresponding to 67 and 100 % of the assumed values.¹

In hadronic models, SDCs can typically only be satisfied by infinite towers of resonances. The estimate of their effects in [4] was based on a Regge model of excited pseudoscalars subjected to available experimental constraints [8, 9], although in the chiral limit excited pseu-

doscalars decouple from the axial anomaly responsible for the longitudinal Melnikov-Vainshein SDC; the alternative of excited axial vector mesons was not considered because of technical difficulties and sparse experimental data. However, in [20, 21] it was shown that in chiral bottom-up holographic QCD (hQCD) models the longitudinal SDC is naturally satisfied by the infinite tower of axial-vector mesons. Remarkably, the short-distance behavior of their transition form factors (TFFs) obtained in [20] agrees exactly with the recently derived asymptotic behavior in a light-cone expansion [22] in analogy to the Brodsky-Lepage limit of the TFF of pseudoscalars, for which such an agreement was noted already in [23]. In the case of the individual TFFs, it is the infinite tower of vector resonances of holographic models which is responsible for this feature, while for the complete HLBL four-point function, the infinite tower of axial vector mesons is required for satisfying the longitudinal SDC. While the simplest chiral hQCD models involve only Goldstone bosons and no excited pseudoscalars, also in the slightly more complicated models that admit massive pions, it was found that the longitudinal SDC is saturated by the tower of axial vector mesons as opposed to the tower of excited pseudoscalars [24].

In [25] we have employed the model of Katz and Schwartz (KS) [26–28], where in addition to quark masses the effects of the $U(1)_A$ anomaly are incorporated, to extend the numerical predictions of flavor-symmetric hard-wall hQCD models to the contributions of the heavier $\eta^{(\prime)}$ mesons (with a pseudoscalar glueball mixing in) and $f_1^{(\prime)}$ axial vector mesons together with their radial excitations. By including a gluon condensate as one further parameter and accounting for gluonic corrections to the asymptotic behavior of TFFs, we have found that the masses of all pseudo-Goldstone bosons as well as their

¹ The 100% uncertainty in the axial-vector contribution is due to the fact that conventional hadronic models [5, 15–19] disagree even in the order of magnitude, with some of them yielding contributions above 10^{-10} , some less than 10^{-11} .

two-photon couplings can be reproduced at the percent level, yielding a_μ contributions in complete agreement with the WP2020 estimate. In this particular hQCD model, the contributions from the axial-vector and excited pseudoscalar towers amounted to 30.5×10^{-11} and 1.6×10^{-11} , respectively, somewhat reducing the previous flavor-symmetric hard-wall result $\sim 40 \times 10^{-11}$, to be compared with the WP2020 estimate of $21(16) \times 10^{-11}$ for axial-vector plus SDC contributions.

However, while the octet-singlet mixing in the pseudoscalar sector and the resulting photon couplings predicted by the KS model are very close to experimental data, the predicted mixing of f_1 and f'_1 axial vector mesons is rather far from experimental findings, pointing to the need of further refinements. Adopting some parts of the construction of improved hQCD models in [29, 30], in this paper we consider a simple hard-wall hQCD model where both flavor and axial anomalies are implemented by a Chern-Simons action that follows more closely a string-theoretic setup with brane-antibrane configurations. Besides a somewhat different implementation of the $U(1)_A$ anomaly than in the KS model, this leads to a Chern-Simons action involving the bi-fundamental scalar field corresponding to the open-string tachyon responsible for brane-antibrane merging and thus chiral symmetry breaking. Remarkably, this yields a significantly more realistic description of f_1 - f'_1 mixing, the equivalent photon rates, and the slope parameters of axial-vector TFFs, but at the price of pseudoscalar transition form factors that now overestimate experimental data at non-zero photon virtualities. The resulting HLBL contributions to a_μ are found to be smaller for the axial vector mesons and larger for the pseudoscalars, with rather little changes in the sum total. While not yet a completely satisfying hQCD model, we consider these results as encouraging with regard to the potential of more elaborate string-inspired hQCD models along the lines of Refs. [29, 30] and also as providing an idea of the range of systematic errors of current hQCD results for the HLBL contribution to the muon $g - 2$.

This paper is organized as follows. In Sec. 2 we give a brief introduction to the tachyon condensation models of [29, 30] which are inspired by brane-antibrane constructions in string theory. In Sec. 3 we describe explicitly the HW AdS/QCD model with relevant parts of the scalar-extended Chern-Simons term included, before detailing the equations of motion and the normalizations for its solutions for both pseudoscalar and axial vector resonances in Sec. 4. In Sec. 5 and 6, we discuss and evaluate the resulting TFFs and also the decay rate of axial vector mesons in electron-positron pairs, which has been proposed in Ref. [31] as an indirect check of doubly virtual axial-vector TFFs. We also discuss briefly scalar mesons, which in the simplest HW AdS/QCD models do not participate in the HLBL scattering amplitude but for which the tachyon-condensation models suggest a specific form of photon interactions. Finally, we present numerical results for the various HLBL contributions to a_μ ,

comparing the different $N_f = 2 + 1$ hQCD models with $U(1)_A$ anomaly.

In the appendices, we describe an important matching factor and the explicit forms appearing in the Chern-Simons term in detail, and we provide details on scalar TFFs.

II. BRANE ANTI-BRANE SYSTEMS AND SUPERCONNECTIONS

In this section we briefly review some features of Dp - \overline{Dp} systems in the context of holography, closely following [29]. We describe some features of the resulting open-string tachyon condensation models and focus in particular on the Chern-Simons term, which we will subsequently include in a simple bottom-up hard-wall (HW) AdS/QCD model.

The string-theoretic construction is based on a configuration of N_c Dq branes intersecting with N_f Dp and N_f \overline{Dp} branes in type IIA or type IIB string theory. In the large N_c ('t Hooft) limit, the color branes are described by background values of the massless string fields (including the graviton), while the flavor branes (which all sit on top of each other) are treated as non-backreacting probe branes. This yields a dual gauge theory with gauge group $SU(N_c)$ with matter in the fundamental representation and a global symmetry group of $U(N_f)_L \times U(N_f)_R$, whose $U(1)_A$ part will be broken by an anomaly. The fields localized to the flavor branes will be a $U(N_f)_L \times U(N_f)_R$ gauge field (A_L, A_R) and a complex scalar field T in the bi-fundamental representation of the gauge group.

The low-energy effective action contains a tachyonic mass term for T associated with the annihilation of Dp and \overline{Dp} branes into lower dimensional strings and branes, which (at least in flat space) is given by $m_T^2 = -1/(2\alpha')$, with α' being the fundamental string tension. In order to interpret the scalar as the dual field of the quark condensate operator $\overline{\psi}_L \psi_R$, its mass has to be set to $m_T^2 = -3/R^2$; hence, the AdS radius R has to satisfy $R^2 = 6\alpha'$. This of course signals a breakdown of the supergravity approximation, which will nevertheless be taken as the basis of constructing a phenomenological bottom-up model for QCD.

Holographic QCD models from tachyon condensation [32, 33] (and their extensions to the Veneziano limit [30, 34]) are obtained by prescribing an AdS-like background, setting $R^2 = 6\alpha'$ and ignoring all higher string theory modes (or including their effects in various different effective potentials). They are semiclassically self-consistent, and the scalar T obtains a stable background value (i.e. condenses), which describes chiral symmetry breaking in the boundary theory.

These models contain a particularly interesting generalization of the usual Chern-Simons term that involves a

superconnection.² The world-volume action of the flavor and anti-flavor branes splits into two parts, $S = S_{DBI} + S_{CS}$, where the Chern-Simons part is given by

$$S_{CS} = T_p \int_{\Sigma_{p+1}} C \wedge \text{Str} \exp[i2\pi\alpha' \mathcal{F}] \quad (1)$$

with

$$i\mathcal{F} = \begin{pmatrix} iF_L - T^\dagger T & DT^\dagger \\ DT & iF_R - TT^\dagger \end{pmatrix}, \quad (2)$$

$$C = \sum_n (-i)^{\frac{p-n+1}{2}} C_n.$$

Here C is a formal sum of Ramond-Ramond (RR) n -form potentials C_n and the integral is supposed to pick the $(p+1)$ -form part of the integrand.

Contrary to the DBI action, the Chern-Simons action can be derived from boundary string field theory to all orders in α' [37, 38]. The above structure actually has a very geometric origin in Quillen's theory of superconnections on \mathbb{Z}_2 graded vector bundles [39]. \mathcal{F} is known as the curvature of the superconnection \mathcal{A} and the multiplication implicit in the definition of the exponential is a \mathbb{Z}_2 generalization of the usual matrix multiplication. A useful aspect of Quillen's results is that when the bundle is trivial (which we will assume in the rest of the paper) $\text{Str} \exp[i2\pi\alpha' \mathcal{F}] = id\Omega$ is a total derivative. In the setup of [29], the color branes generate an RR flux proportional to N_c , which gets picked up by the 5 form part Ω_5 . After effectively reducing dimensionally to AdS_5 , there is a quadratic coupling of the C_3 RR potential and the fields contained in Ω_1 ; this is responsible for the correct implementation of the $U(1)_A$ anomaly. Hence, the two most important terms from the Chern-Simons action will be

$$T_p \int_{AdS_5} C_3 d\Omega_1 + \frac{N_c}{(2\pi)^2} \frac{1}{(2\pi\alpha')^3} \int_{AdS_5} \Omega_5. \quad (3)$$

In the following section we implement this structure into a hard-wall (HW) hQCD model. While the first term is subleading in N_c , it plays an important role phenomenologically, as it will be responsible for the large mass of the η' meson.

III. HARD-WALL ADS/QCD MODEL WITH SCALAR-EXTENDED CHERN-SIMONS TERM

Upon expanding the DBI action of the tachyon condensation models, one obtains in lowest order of α' exactly the action of the original HW AdS/QCD models of Ref. [40, 41] which are known to be well suited for the

description of low lying mesons. The tachyon T can be identified with the bi-fundamental scalar X of the HW models. There is, however, an important factor that determines the interactions in the Chern-Simons term involving the scalar fields. The relation, which is derived in Appendix A, is

$$T = X^\dagger g_5 \sqrt{\frac{\pi}{2}}, \quad (4)$$

where g_5 is the 5-dimensional Yang-Mills coupling of flavor gauge fields and X is a bi-fundamental scalar field dual to bilinear quark operators. Since the tachyon has dimension 1 and g_5 has mass dimension $-\frac{1}{2}$, we obtain the correct mass dimension for X , namely $\frac{3}{2}$.

In bottom-up HW models, the background geometry is simply pure AdS_5 , which (upon setting the AdS radius equal to 1) has a metric

$$ds^2 = z^{-2}(\eta_{\mu\nu} dx^\mu dx^\nu - dz^2), \quad (5)$$

in Poincaré coordinates. Confinement and conformal symmetry breaking is implemented by a sharp cutoff at $z = z_0$, where one has to specify boundary conditions for the fields.

The complete action relevant to the processes that we will consider later reads

$$S = -\frac{1}{4g_5^2} \int_{AdS_5} \sqrt{g} \text{tr} [(F_L)_{MN} (F_L)^{MN} + (F_R)_{MN} (F_R)^{MN}]$$

$$+ \int_{AdS_5} \sqrt{g} \text{tr} [D_M X D_N X^\dagger g^{MN} + 3X X^\dagger]$$

$$+ \frac{N_c}{(2\pi)^2} \frac{1}{(2\pi\alpha')^3} \int_{AdS_5} \Omega_5$$

$$+ \int_{AdS_5} \frac{1}{2B(z)} dC_3 * dC_3 + T_p \int_{AdS_5} C_3 d\Omega_1, \quad (6)$$

where it is understood that we replace α' by $\frac{1}{6}$ and any occurrence of T in the Chern-Simons terms has to be replaced by (4). The first three integrals are identical to the usual HW action upon setting $T = 0$ in Ω_5 .

In the AdS geometry, the scalar field X admits a background of the form

$$X_0 = \frac{1}{2}(mz + \sigma z^3) = \frac{1}{2} \begin{pmatrix} v_q & & \\ & v_q & \\ & & v_s \end{pmatrix}, \quad (7)$$

where the matrices m, σ are proportional to the quark masses and the chiral condensate in the dual theory. We will restrict to $N_f = 3$, with $m_u = m_d \neq m_s$ but uniform $\sigma \propto \mathbf{1}$. These parameters together with z_0, g_5 will be fitted to π_0, ρ_0, K^0 and OPE data below.

The fluctuations around the vacuum of the scalar and the longitudinal gauge fields describe scalar and pseudoscalar mesons, while the transverse degrees of freedom of the gauge fields describe vector and axial-vector

² This generalization has been recently shown to be the appropriate framework for a wider class of anomalies including also systems with interfaces and spacetime boundaries [35, 36].

mesons. We parametrize the pseudoscalar fluctuations of X as [42]

$$X = e^{i\eta} X_0 e^{i\eta}, \quad \eta = \eta^a(x, z) t^a, \quad a = 0, \dots, 8 \quad (8)$$

where $\text{tr}(t^a t^b) = \delta^{ab}/2$.

In (6) we have included a phenomenological background field $B(z)$ in the kinetic term of the RR 3-form, which will eventually account for the running of the QCD coupling in the gluon condensate. Some explicit expressions for Ω_1, Ω_5 relevant for our discussion are given in a separate appendix. It is possible to dualize the last line of (6) to

$$S_a = \int \frac{1}{2} B(z) (da - T_p \Omega_1) * (da - T_p \Omega_1), \quad (9)$$

where a can be interpreted as a pure pseudoscalar glueball field (before its eventual mixing with pseudoscalar mesons). Note that Ω_1 is only defined up to an extra closed term with integer periods $\Omega_1 \rightarrow \Omega_1 + \xi$. These are exactly the gauge symmetries of a circle-valued scalar, so this action is well-defined. As is shown in the appendix, to leading order in pseudoscalar fluctuations,

$$\Omega_1 = 2\pi\alpha' \text{tr} \left(2\eta d \exp(-2\pi\alpha' T_0^2) + (A_L - A_R) \exp(-2\pi\alpha' T_0^2) \right). \quad (10)$$

Upon rescaling³ a by a factor of $4\pi\alpha' T_p$, one arrives at

$$S_a = \frac{1}{2} \tilde{B}(z) (da - \tilde{\Omega}_1) \wedge * (da - \tilde{\Omega}_1) \quad (11)$$

with

$$\tilde{\Omega}_1 = \text{tr} \left(\eta d \exp(-2\pi\alpha' T_0^2) + A \exp(-2\pi\alpha' T_0^2) \right), \quad (12)$$

$$A = \frac{A_L - A_R}{2}. \quad (13)$$

The action in terms of the components of the field can be written as

$$\frac{\tilde{B}(z)}{2} \sqrt{g} g^{MN} (\partial_M a - \text{tr}(V_t A_M + \eta \partial_M V_t)) \times (\partial_N a - \text{tr}(V_t A_N + \eta \partial_N V_t)) \quad (14)$$

with $V_t = \exp(-2\pi\alpha' T_0^2)$. Upon expanding this action at small z we find

$$\mathcal{L}_a = \frac{(\tilde{B}(z) \frac{N_f}{2})}{2} \sqrt{g} g^{MN} (\partial_M \tilde{a} - A_M^0) (\partial_N \tilde{a} - A_N^0) \quad \text{with } \tilde{a} = a \sqrt{2/N_f}. \quad (15)$$

³ Since a is a circle-valued scalar, this rescaling would affect the normalization of its periods. We are however not interested in situations with nonzero winding.

This is, asymptotically, of the same form as the action of the KS model [26], with $\sqrt{\tilde{B}(z) \frac{N_f}{2}}$ identified with

$$\tilde{Y}_0 = \frac{C_0}{-\ln z \Lambda} - \Xi_0 z^4 \left((\ln z \Lambda) - \frac{1}{2} + \frac{1}{8 \ln z \Lambda} \right) \quad (16)$$

of [25]. As explained in that paper, a fit to the OPE of QCD forces the leading part of \tilde{Y}_0 to be proportional to the running coupling α_s . The subleading part is a consequence of the demanding consistency of the EOM of [25]; it allows us to include a non-zero gluon condensate, parametrized by Ξ_0 , and we will take over this explicit form to the present model.

IV. EQUATIONS OF MOTION AND MESON MODES

We first list the quadratic part of the action and the equations of motion for the pseudoscalar sector that follow from it. The pseudoscalar action for the $a = 8, 0$ subsector reads

$$\begin{aligned} \mathcal{L}_2 \supset & \frac{-1}{4g_5^2 z} (\partial_M A_N^a - \partial_N A_M^a)^2 \\ & + \frac{M_{ab}^2}{2z^3} (\partial_M \eta^a - A_M^a) (\partial_M \eta^b - A_M^b) \\ & + \frac{\tilde{B}}{2z^3} \left(\partial_M a - \text{tr}\{A_M V_t + \eta \partial_M V_t\} \right)^2, \end{aligned} \quad (17)$$

where the spacetime indices are contracted with the 5d Minkowski metric and

$$M_{ab}^2 = \frac{1}{3} \begin{pmatrix} 2v_q^2 + v_s^2 & \sqrt{2}(v_q^2 - v_s^2) \\ \sqrt{2}(v_q^2 - v_s^2) & v_q^2 + 2v_s^2 \end{pmatrix}. \quad (18)$$

Flavor traces of the tachyon potential $V_t = \exp(-\pi^2 g_5^2 \alpha' X_0^2)$ will be written as

$$\text{tr}(t^a V_t) = W^a. \quad (19)$$

In the following we will work in the $A_z = 0$ gauge. The pseudoscalar fluctuations of the gauge field are parametrized as $A_\mu^a = \partial_\mu \varphi^a$. The equations of motion in the pseudoscalar sector for $a = 0, 8$ read

$$\begin{aligned} \partial_z \left(\frac{1}{z} \partial_z \varphi^a \right) + g_5^2 \frac{M_{ab}^2}{z^3} (\eta^b - \varphi^b) + g_5^2 \frac{\tilde{B}}{z^3} (a - \varphi^b W^b) W^a &= 0, \\ \partial_z \left[\frac{\tilde{B}}{z^3} (\partial_z a - \eta^a \partial_z W^a) \right] + q^2 \frac{\tilde{B}}{z^3} (a - \varphi^a W^a) &= 0, \\ \partial_z \left(\frac{M_{ab}^2}{z^3} \partial_z \eta^b \right) + q^2 \frac{M_{ab}^2}{z^3} (\eta^b - \varphi^b) \\ &+ \frac{\tilde{B}}{z^3} (\partial_z a - \eta^b \partial_z W^b) \partial_z W^a = 0, \\ -\frac{q^2}{g_5^2} \frac{1}{z} \partial_z \varphi^a + \frac{\tilde{B}}{z^3} (\partial_z a - \eta^b \partial_z W^b) W^a + \frac{M_{ab}^2}{z^3} \partial_z \eta^b &= 0. \end{aligned} \quad (20)$$

In these equations a sum over the index b is understood. The last equation is the A_z equation of motion.

The $a = 3$ sector is not affected by the addition of S_a , which implements the $U(1)_A$ anomaly; the corresponding fluctuation equations are the same as in [24].

An important point is the choice of boundary conditions. After varying the action, the boundary term that has to vanish at $z = 0$ and $z = z_0$ is

$$\begin{aligned} \frac{q^2}{g_5^2} \frac{1}{z} \partial_z \varphi^a (\delta \varphi^a) - \frac{\tilde{B}}{z^3} (\partial_z a - \eta^b \partial_z W^b) \delta a \\ - \frac{M_{ab}^2}{z^3} \partial_z \eta^b \delta \eta^a = 0, \end{aligned} \quad (21)$$

which upon using the A_z equation of motion reads

$$\begin{aligned} \frac{q^2}{g_5^2} \frac{1}{z} \partial_z \varphi^a (\delta \varphi^a - \delta \eta^a) \\ - \frac{\tilde{B}}{z^3} (\partial_z a - \eta^b \partial_z W^b) (\delta a - W^a \delta \eta^a) = 0. \end{aligned} \quad (22)$$

In the rest of the paper we will be choosing so-called [24] HW3 boundary conditions at $z = z_0$, i.e. $\varphi^a = \eta^a$, supplemented by $a = W^b \eta^b$.

In order to compute correlation functions of operators or masses and decay constants of particles in the dual gauge theory we need to solve the set of equations (20) subject to the above boundary conditions in the infrared. For the former, one has to supply boundary conditions in the UV which make the solution non-normalizable, while for the latter, one has to consider normalizable modes. Normalizable modes only exist for discrete values of q^2 which can be identified with the mass squared of a pseudoscalar meson. The inner product from which the norm follows reads

$$\begin{aligned} \langle \Phi_n, \Phi_m \rangle = \int dz \frac{1}{g_5^2} \frac{\partial_z \varphi_n^a \partial_z \varphi_m^a}{z} + \frac{M_{ab}}{z^3} (\eta_n^a - \varphi_n^a) (\eta_m^b - \varphi_m^b) \\ + \frac{\tilde{B}}{z^3} (a_n - \varphi_n^a W^a) (a_m - \varphi_m^b W^b). \end{aligned} \quad (23)$$

The decay constants are defined as in [25] and read

$$f_n^a = -g_5^{-2} \partial_z \varphi_n^a / z \Big|_{z \rightarrow 0}, \quad (24)$$

$$f_G^n = \tilde{B} \partial_z a_n / z^3 \Big|_{z \rightarrow 0}. \quad (25)$$

The equations of motion for the $a = 0, 8$ axial vector mesons read

$$-\partial_z \left(\frac{1}{z} \partial_z \xi^a \right) - \frac{q^2}{z} \xi^a + g_5^2 \frac{M_{ab}^2}{z^3} \xi^b + g_5^2 \frac{\tilde{B}}{z^3} W^a W^b \xi^b = 0. \quad (26)$$

Their norm is given by

$$1 = \int dz \frac{1}{g_5^2 z} \xi^a \xi^a. \quad (27)$$

and the decay constants are computed by

$$F_n^a = -g_5^{-2} \partial_z \xi_n^a / z \Big|_{z \rightarrow 0}. \quad (28)$$

A. Parameter settings

The HW AdS/QCD model with scalar-extended Chern-Simons terms thus constructed will be referred to as CS' in the following. We shall also consider a variant CS', where the tachyon T is only appearing in Ω_1 , which implements the $U(1)_A$ anomaly, but where Ω_5 involves only flavor gauge fields.⁴ These two models will be compared with the version of the KS model evaluated by us in [25], to which we refer for detailed tables of numerical results. All three models, for which we take $m_u = m_d \neq m_s$ and $\sigma \propto \mathbf{1}$, have the same number of free parameters, which will be fixed by $f_\pi = 92.21$ MeV, $m_\rho = 775.556$ MeV,

$$\begin{aligned} m_K^2 &= \frac{1}{2} (m_{K^\pm}^2 + m_{K^0}^2) - \frac{1}{2} (m_{\pi^\pm}^2 - m_{\pi^0}^2) \\ &= (495.007 \text{ MeV})^2 \end{aligned} \quad (29)$$

and a least-square fit of m_η and $m_{\eta'}$.

The coupling constant g_5 is usually fixed by the OPE of the vector current correlator as

$$g_5^2 = 12\pi^2 / N_c = (2\pi)^2 \quad (\text{OPE fit}), \quad (30)$$

but we shall alternatively consider matching the decay constant of the ρ meson, which in the HW model leads to [43]

$$g_5^2 = 0.894 (2\pi)^2 \quad (F_\rho\text{-fit}). \quad (31)$$

The latter in fact significantly improves the holographic result for the hadronic vacuum polarization [43], and such an $\approx 10\%$ reduction of g_5^2 is also warranted by comparing with next-to-leading order QCD results for the vector correlator at moderately large Q^2 values [13, 44, 45].

B. Scalar mesons

Scalar mesons are naturally present in this model as scalar fluctuations of the field X . With just the terms quadratic in X included in (6), the spectrum will be flavor symmetric and there is no coupling to two photons for the $a = 0, 3, 8$ mesons.⁵

However, if one introduces tachyon potentials also in the Yang-Mills action, as done in the improved hQCD

⁴ In the $a = 3$ sector, the CS' model is in fact identical to the HW3 model considered in [24].

⁵ The string-theoretic motivation of AdS/QCD models also suggests flavor-singlet scalar and tensor mesons in the form of dilaton and metric fluctuations dual to glueball modes, which inevitably have two-photon couplings from vector-meson dominance. In the Witten-Sakai-Sugimoto model, their contributions to a_μ have been estimated [46] to be below the level of 10^{-12} . In [47], metric fluctuations have been used as a model for tensor mesons in general (with adjusted coupling strength), even though they do not naturally form flavor multiplets.

models of Ref. [29, 32–34, 48, 49], one obtains additional terms such as

$$-\gamma \frac{g_5^2 \pi^2}{4} \sqrt{g} \text{tr}((XX^\dagger)^2), \quad (32)$$

which after expanding $X = X_0 + S$ break the flavor symmetry of the excitations and introduce quark mass effects to the spectrum, and

$$\gamma \frac{\pi^2 \alpha'}{4} \sqrt{g} \text{tr}(X^\dagger X F_L^2 + X X^\dagger F_R^2), \quad (33)$$

which leads to a nonzero TFF. We have introduced here by hand the phenomenological parameter γ in front of both terms, whose deviation from 0 measures how much our model differs from the original action (6); $\gamma = 1$ corresponds to keeping the terms of order α' from (A2) in the Yang-Mills action.

The mode equations for $S_n = S_n^a t^a$ are

$$z^5 \partial_z \frac{1}{z^3} \partial_z S_n + (zm_n)^2 S_n + \left(3 - \frac{6g_5^5 \pi^2 \gamma X_0^2}{4}\right) S_n = 0, \quad (34)$$

subject to boundary conditions $S(z_0) = 0$ and $S(\varepsilon) \sim \varepsilon^3$ for small ε . The normalization is

$$\int_0^{z_0} dz \frac{S_n^a S_n^a}{z^3} = 1, \quad (35)$$

where the sum over a is understood.

The masses that are obtained for such scalars are, however, too large to be identified with the scalar mesons $f_0(500)$, $a_0(980)$, and $f_0(980)$, which are of predominant interest for the HLBL contribution. In fact, those are likely tetraquark states and thus presumably beyond a holographic description in the large- N 't Hooft limit. With $\gamma = 1$ and g_5 as in (30), the $a = 3, 8, 0$ scalar masses are 1.722, 1.722, and 2.084 GeV; with reduced coupling (31) slightly smaller: 1.610, 1.610, and 2.006 GeV. We thus do not consider them any further here, because with these parameters they contribute negligibly to a_μ (only $\lesssim 10^{-12}$). We provide, however, some additional pertinent comments on their TFFs in Appendix C.

V. TRANSITION FORM FACTORS

Using the expressions for Ω_5 derived in the appendix, we can obtain the transition form factors for the pseudoscalar mesons (\mathcal{Q} is the quark charge matrix)

$$\begin{aligned} F(Q_1^2, Q_2^2) = & -\frac{N_c}{2\pi^2} \frac{1}{3} \int dz \text{tr} \mathcal{Q}^2 \\ & \times \left\{ e^{-2\pi\alpha' T_0^2} [2\varphi' \mathcal{J}_1 \mathcal{J}_2 - \varphi(\mathcal{J}_1 \mathcal{J}_2)'] \right. \\ & \left. + 2(e^{-2\pi\alpha' T_0^2})' \varphi \mathcal{J}_1 \mathcal{J}_2 \right\} \\ & + \frac{N_c}{2\pi^2} \int dz \text{tr} (e^{-2\pi\alpha' T_0^2})' \mathcal{Q}^2 \eta \mathcal{J}_1 \mathcal{J}_2, \quad (36) \end{aligned}$$

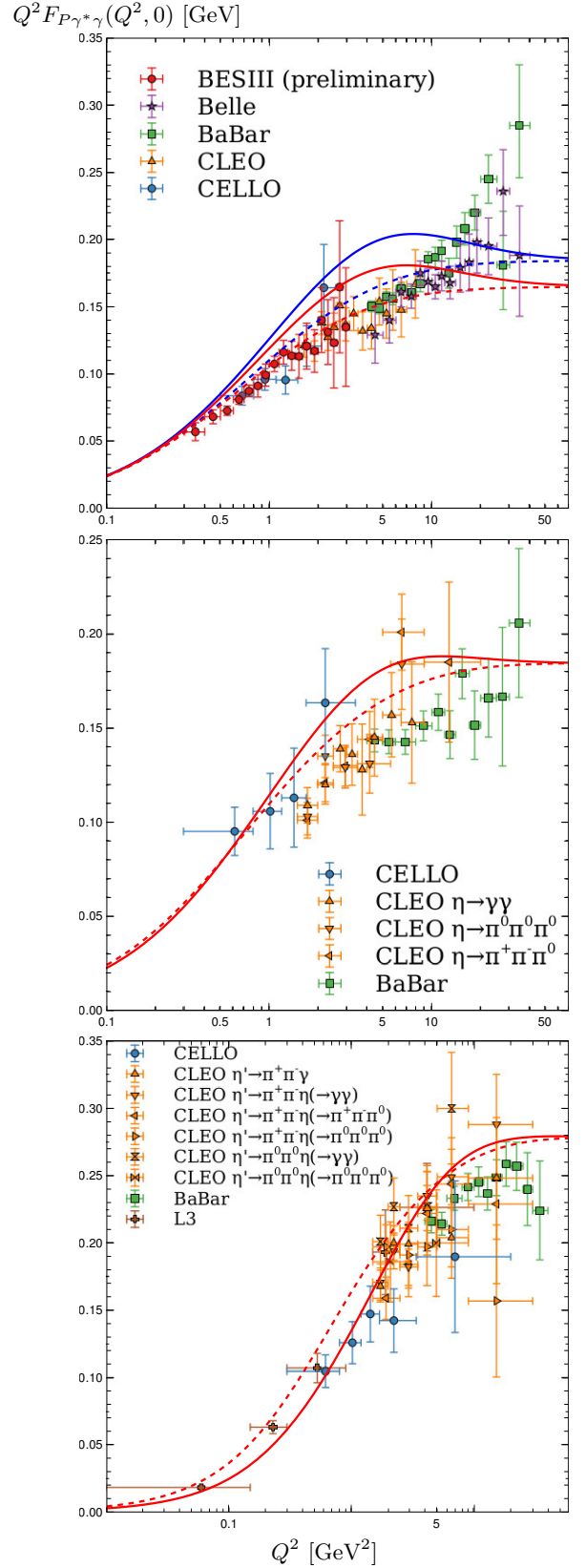


FIG. 1. Singly virtual TFF $Q^2 F(Q^2, 0)$ for π^0 , η and η' with fully scalar extended CS term (CS'', full lines) and with scalars omitted in Ω_5 (CS', dashed line), plotted on top of experimental data as compiled in Fig. 54 of Ref. [4]. Red lines correspond to a reduced coupling g_5 (F_ρ fit), blue ones to the OPE value (only included for the experimentally better constrained π^0 TFF).

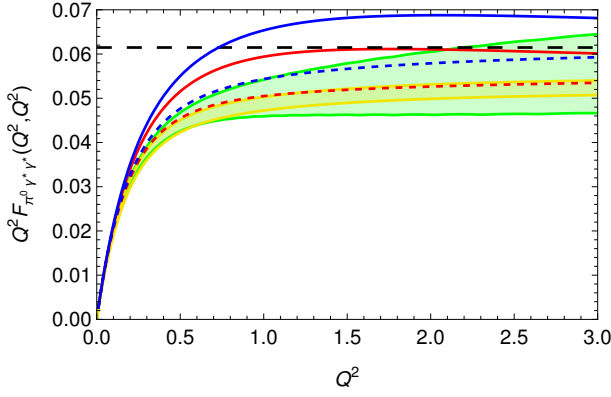


FIG. 2. Doubly virtual $F_{\pi^0 \gamma^* \gamma^*}$ with scalar extended CS term (CS'', full line) and with scalars omitted in Ω_5 (CS', dashed line), both with OPE fit (blue) and reduced g_5 (F_ρ fit, red) in comparison with dispersive result of Ref. [50] (green band) and the lattice result of Ref. [51] (yellow band). The horizontal black dashed line indicates the BL limit.

where $\mathcal{J}_{1,2}$ is the bulk-to-boundary vector propagator

$$\mathcal{J}(Q_i, z) = Q_i z \left[K_1(Q_i z) + \frac{K_0(Q_i z_0)}{I_0(Q_i z_0)} I_1(Q_i z) \right] \quad (37)$$

for photon virtualities $Q_{1,2}^2$ and the prime denotes differentiation with respect to z . Partial integration yields

$$F(Q_1^2, Q_2^2) = -\frac{N_c}{2\pi^2} \int dz \operatorname{tr} Q^2 \left\{ e^{-2\pi\alpha' T_0^2} \varphi' \mathcal{J}_1 \mathcal{J}_2 + (e^{-2\pi\alpha' T_0^2})' (\varphi - \eta) \mathcal{J}_1 \mathcal{J}_2 \right\}, \quad (38)$$

up to total derivatives which we cancel by a suitable boundary term. The quantity Ω_5 is only determined up to exact terms $d\kappa$ anyway and we use that freedom to cancel the boundary term in the above equation. Doing so, the resulting TFFs satisfy a sum rule that will be derived below.

For $F(0, 0)$, which determines the coupling to two real photons, we can derive sum rules similarly to [24] but with certain modifications. For those we will need particular non-normalizable modes Φ_q , which are solutions to the equations of motion for arbitrary q^2 . Those exist only if we allow for more general boundary conditions in the UV. The IR boundary conditions are unchanged. We first note that the inner product of Φ_q and a normalizable mode Φ_n reduces to a boundary contribution.

$$\begin{aligned} \langle \Phi_n, \Phi_q \rangle (q^2 - m_n^2) = \\ -(\eta^a - \varphi^a) \frac{M_{ab}^2}{z^3} \partial_z \eta_n^b|_\varepsilon - (a - \varphi^a W^a) \frac{\tilde{B}}{z^3} (a'_n - \eta_n^b W^b)|_\varepsilon. \end{aligned} \quad (39)$$

For modes $\eta^0 \rightarrow 1, a \rightarrow W^0(0)$ (and all other functions going to zero) the RHS becomes $m_n^2 f_n^0$. If we let $\eta^8 \rightarrow 1, a \rightarrow W^8(0) = 0$ and the other functions to zero

then the RHS becomes $m_n^2 f_n^8$. We label these two different choices of boundary conditions by a lowercase (bracketed) flavor index and focus on the solution for $q^2 = 0$, which we denote by $\Phi_{(a)}$. This solution will be relevant for the sum rule for the TFF and we now want to show that η^a are constants in that case. For $q^2 = 0$, the equations of motion imply

$$\frac{\tilde{B}}{z^3} (a' - \eta^b W^b) = \beta, \quad (40)$$

$$\frac{M_{ab}^2 \eta'^b}{z^3} = -\beta W^a, \quad (41)$$

for an as-of-yet undetermined constant β . The solution of these equations is

$$\eta_{(c)}^a = \delta_c^a - \beta \int_0^z d\tilde{z} \tilde{z}^3 (M_{ab}^2)^{-1} W^b, \quad (42)$$

$$a_{(c)} = W^c(0) + \int_0^z d\tilde{z} \left(\beta \frac{\tilde{z}^3}{\tilde{B}} + \eta_{(c)}^b W^b \right), \quad (43)$$

where η of the first line is inserted into the second line. The first terms in each line are constants and are determined by the UV boundary conditions. The φ^a functions can be obtained from the above η^a and a . Using the explicit expressions in the two equations above one can see that the IR boundary condition $a(z_0) = \eta^a(z_0) W^a(z_0)$ is satisfied for $\beta = 0$. This means that η^0, η^8 are constant and fully determined by the boundary condition at $z = 0$.

With $Z^a = \operatorname{tr}(e^{-2\pi\alpha' T_0^2} Q^2 t^a)$ the TFF (38) at vanishing momenta reads (after using $\varphi_n^a(z_0) = \eta_n^a(z_0)$)

$$F_n(0, 0) = \frac{N_c}{2\pi^2} \int_0^{z_0} dz Z'^a \eta_n^a - \frac{N_c}{2\pi^2} (Z^a \eta_n^a)|_{z_0}, \quad (44)$$

hence, after multiplying by $\frac{f_n^a m_n^2}{q^2 - m_n^2}|_{q^2=0}$ and summing over all modes, we can replace the normalizable mode with the non-normalizable mode. Then the following equation is obtained

$$\sum_n F_n(0, 0) f_n^a = \frac{N_c}{2\pi^2} \operatorname{tr}(Q^2 t^a). \quad (45)$$

By splitting φ into $\varphi^0 t^0 + \varphi^8 t^8$ and similar for η we can split the TFF into two parts $F(q_1, q_2) = \bar{F}^0(q_1, q_2) + \bar{F}^8(q_1, q_2)$. To better facilitate numerical comparison with the previous analysis [25], we define $F^a = \bar{F}^a / \operatorname{tr}(t^a Q^2)$ so that $F(q_1, q_2) = \sum_a \operatorname{tr}(t^a Q^2) F^a(q_1, q_2)$.

Using this decomposition we have at zero momentum

$$\bar{F}_n^a(0, 0) = \frac{N_c}{2\pi^2} \int_0^{z_0} dz Z'^a \eta_n^a - \frac{N_c}{2\pi^2} (Z^a \eta_n^a)|_{z_0} \quad (46)$$

with no sum over a on the RHS. The sum rule from before can then be generalized to (no summation over a or b)

$$\sum_n \bar{F}_n^a(0, 0) f_n^b = \frac{N_c}{2\pi^2} \delta^{ab} \operatorname{tr}(Q^2 t^a) \quad (47)$$

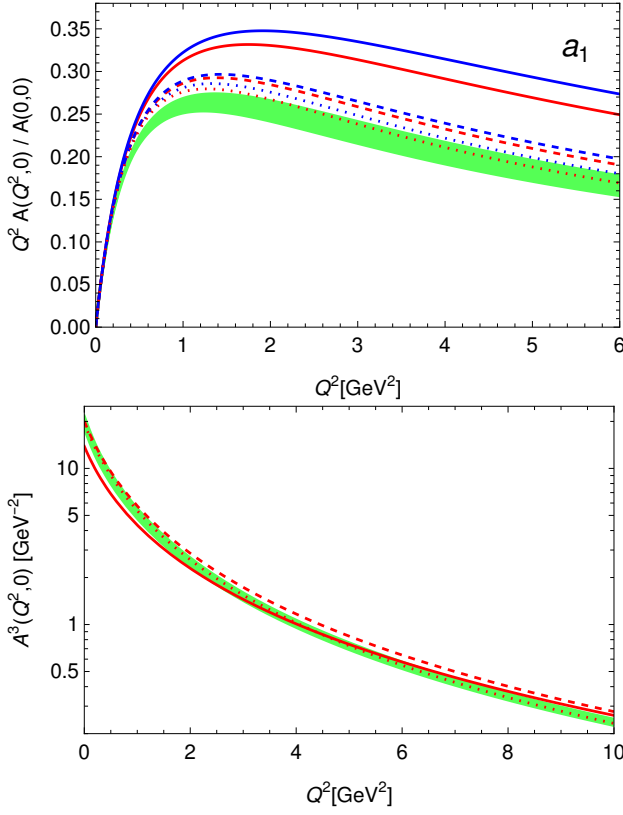


FIG. 3. The singly virtual a_1 TFF $A^3(Q^2, 0)$ in the various models (CS $''$, full lines; CS $'$ dashed lines, KS dotted lines) and for different coupling g_5 (blue: OPE fit, red: F_ρ fit) in comparison to the dispersive result (green band) of Ref. [52]. The upper panel shows the normalized TFF $Q^2 A(Q^2, 0)/A(0, 0)$, the lower panel the unnormalized $A^3(Q^2, 0)$, restricted to the reduced coupling g_5 obtained by the F_ρ fit. Here the dotted line representing KS(F_ρ -fit) lies within the error band of the dispersive result for all values of Q^2 .

For axial-vector mesons, we use the following parametrization⁶ for the amplitude to decay into two virtual photons

$$\mathcal{M}^{\mu\nu\alpha} = -i \frac{N_c}{4\pi^2} \left(\varepsilon^{\mu\nu\rho\alpha} (q_2)_\rho (q_1^2 \delta_\mu^\nu - q_1^\mu (q_1)_\nu) A_n(Q_1^2, Q_2^2) - \varepsilon^{\mu\nu\rho\alpha} (q_1)_\rho (q_2^2 \delta_\mu^\nu - q_2^\mu (q_2)_\nu) A_n(Q_2^2, Q_1^2) \right), \quad (48)$$

where $Q^2 = -q^2$. The function A is determined by the Chern-Simons term and reads

$$A(Q_1^2, Q_2^2) = \frac{2}{Q_1^2} \int \text{tr} Q^2 e^{-2\pi\alpha' T_0^2 \xi} \mathcal{F}_1' \mathcal{J}_2. \quad (49)$$

Below we will use the same flavor decomposition for the axial-vector TFF as for the pseudoscalar TFF.

⁶ Up to an overall factor $N_c m_A^2 / (4\pi^2)$, the asymmetric functions $A(q_1^2, q_2^2)$ corresponds to the structure function \mathcal{F}_2 of Ref. [22, 31], whereas the structure function \mathcal{F}_1 vanishes in the hQCD models.

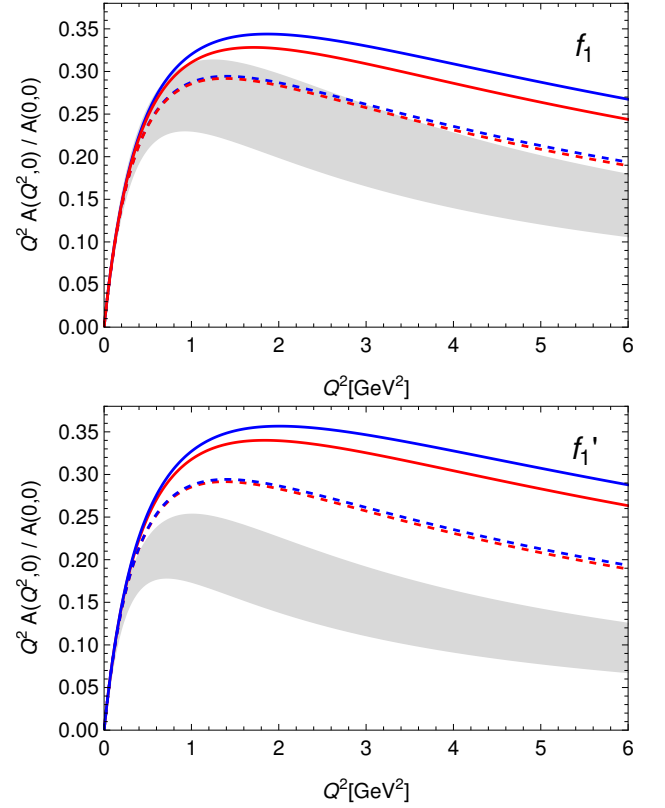


FIG. 4. Singly virtual TFF $Q^2 A(Q^2, 0)/A(0, 0)$ for f_1 and f_1' (CS $''$: full lines, CS $'$: dashed lines, OPE fit: blue, F_ρ fit: red) compared to L3 data [53, 54] (shaded areas).

A. Two-photon decays of axial vector mesons

Equation (48) together the result (49), and $\mathcal{J}_1' \sim Q_1^2$ for $Q_1^2 \rightarrow 0$, implies that an axial vector meson cannot decay into two real photons. One can, however, define an equivalent two-photon rate by the approach to zero, which in the notation of [22, 31] reads

$$\tilde{\Gamma}_{\gamma\gamma} = \frac{\pi\alpha^2 m_A}{48} |\mathcal{F}_s(0, 0)|^2, \quad (50)$$

where

$$\mathcal{F}_s(0, 0) \equiv 3m_A^2 A(0, 0)/(2\pi^2). \quad (51)$$

The experimental results of [53, 54] for the singly virtual TFF of f_1 and f_1' mesons have been parametrized by a dipole ansatz and used in previous evaluations of their contribution to a_μ in [15]:

$$A^{\text{dip.}}(Q_1^2, Q_2^2) = \frac{A^{\text{dipole}}(0, 0)}{(1 + Q_1^2/\Lambda_D^2)^2 (1 + Q_2^2/\Lambda_D^2)^2}, \quad (52)$$

which can be compared with the slope parameter of the singly virtual TFF in our calculation

$$\Lambda = \sqrt{\left. \frac{-2A(Q^2, 0)}{\partial A(Q^2, 0)/\partial Q^2} \right|_{Q^2=0}}. \quad (53)$$

	$g_5^2 = (2\pi)^2$							$g_5^2 = 0.894(2\pi)^2$						
	π^0	π^*	a_1	a_1^*	a_1^{**}	a_1^{***}	a_1^{****}	π^0	π^*	a_1	a_1^*	a_1^{**}	a_1^{***}	a_1^{****}
m	0.135*	1.709	1.429	2.419	3.398	4.388	5.3864	0.135*	1.579	1.3709	2.366	3.3574	4.356	5.360
$f \vee F_A/m_A$	0.09221*	0.0016	0.1945	0.244	0.2911	-0.332	0.3695	0.09221*	0.0019	0.2002	0.257	0.3077	0.351	0.390
$F \vee A^3(0,0)$	0.274	0.1528	13.48	7.16	0.33	-0.014	0.91	0.274	0.1629	13.86	6.56	-0.58	0.49	0.73
$a_\mu \times 10^{11}$	73.3	0.95	4.86	1.65	0.36	0.17	0.11	68.8	1.09	4.93	1.52	0.32	0.17	0.10
$\check{F} \vee \check{A}^3(0,0)$	0.277	0.195	21.24	-0.266	2.08	0.303	0.513	0.277	0.169	20.10	0.53	1.80	0.36	0.47
$\check{a}_\mu \times 10^{11}$	66.6	0.8	8.19	0.84	0.44	0.18	0.11	64.3	0.68	7.59	0.87	0.40	0.17	0.10

TABLE I. Results for pseudoscalar and axial-vector mesons in the isotriplet sector (the gluon condensate parameter Ξ_0 does not play a role here). Quantities marked by $\check{}$ correspond to the CS' model (Ω_5 without extension by the scalar fields in the superconnection). All quantities in units of (powers of) GeV.

	$\Xi_0 = 0.0158$						$\Xi_0 = 0.0177$					
	η	η'	G/η''	$\eta^{(3)}$	$\eta^{(4)}$	$\eta^{(5)}$	η	η'	G/η''	$\eta^{(3)}$	$\eta^{(4)}$	$\eta^{(5)}$
m	0.564	0.944	1.655	1.856	1.904	2.590	0.572	0.934	1.514	1.764	1.883	2.521
$m - m^{\text{exp}}$	3.0%	-1.4%					4.4%	-2.5%				
f^8	0.102	-0.034	0.0053	-0.009	0.027	-0.012	0.103	-0.035	0.0055	-0.03	-0.012	0.030
f^0	0.023	0.100	0.044	0.025	-0.026	-0.0024	0.026	0.105	0.0445	0.040	0.002	-0.012
f_G	-0.029	-0.067	-0.129	-0.069	0.024	0.064	-0.031	-0.070	-0.108	-0.059	0.031	-0.053
$F^8(0,0)$	1.48	-0.39	0.16	-0.207	-0.053	0.86	1.47	-0.433	0.166	-0.136	-0.0287	-0.968
$F^0(0,0)$	0.45	1.26	0.59	-0.556	0.631	0.225	0.426	1.169	0.690	0.128	0.789	0.010
$F(0,0)$	0.265	0.305	0.175	-0.171	-0.167	0.144	0.257	0.276	0.203	0.0218	0.212	-0.09
$F - F^{\text{exp}}$	-3%	-11%					-6%	-20%				
$a_\mu \times 10^{11}$	19.4	14.9	1.97	0.87	1.22	0.16	17.2	12.2	2.6	0.1	1.62	0.12
$\check{F}^8(0,0)$	1.57	-0.37	-0.68	0.65	-0.77	-0.42	1.56	-0.39	-0.64	0.87	0.127	0.35
$\check{F}^0(0,0)$	0.49	1.72	-0.69	-0.032	0.68	-0.18	0.48	1.70	-0.67	-0.53	-0.082	-0.13
$\check{F}(0,0)$	0.284	0.433	-0.253	0.054	0.11	-0.089	0.282	0.423	-0.245	-0.060	-0.010	-0.0015
$\check{F} - F^{\text{exp}}$	+4%	+26%					+3%	+23%				
$\check{a}_\mu \times 10^{11}$	18.7	21.4	0.83	0.17	0.15	0.05	17.7	20.1	0.89	0.03	0.01	0.0003

TABLE II. Results for the isoscalar pseudoscalar sector, with gluon condensate values Ξ_0 , and for two choices of g_5 : $g_5 = 2\pi$ corresponding to matching the vector correlator to the LO UV-behavior in QCD, and the reduced value corresponding to a fit of F_ρ . The quantities F^0, F^8 have been defined in the text below (38). Quantities marked by $\check{}$ correspond to the CS' model (Ω_5 without extension by the scalar fields in the superconnection). All dimensionful quantities in units of (powers of) GeV. The central experimental value F^{exp} is 0.274 and 0.3437 GeV $^{-1}$ for η and η' , respectively, with 3-4% errors according to PDG [55].

B. Electron-positron decay of axial-vector mesons

Axial vector mesons can also decay into an electron-positron pair according to an effective one-loop diagram shown in Fig. 5. The two photons emitted by the spinors couple to the axial vector meson via its TFF. This process is, therefore, a useful window into the doubly virtual axial vector TFF [31].

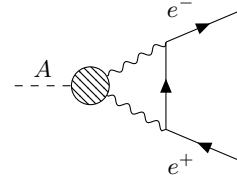


FIG. 5. An axial vector meson decaying into electron and positron via a 1-loop process involving the doubly virtual axial-vector TFF.

Using the decomposition in terms of tensor structures

	$\Xi_0 = 0.0158$		$\Xi_0 = 0.0177$	
	$g_5^2 = (2\pi)^2$		$g_5^2 = 0.894(2\pi)^2$	
	f_1	f_1'	f_1	f_1'
m	1.503	1.625	1.463	1.583
$m - m^{\text{exp}}$	+17%	+13%	+14%	+11%
m^*	2.450	2.547	2.402	2.405
m^{**}	3.425	3.491	3.388	3.450
F_A^8/m_A	0.162	0.108	0.178	0.089
F_A^0/m_A	0.091	-0.139	0.078	-0.154
$A^8(0,0)$	13.37	9.04	14.95	7.61
$A^0(0,0)$	6.88	-10.75	5.75	-11.80
θ_A	62.78°	-40.05°	68.96°	-32.8°
$A(0,0)$	3.16	-2.06	3.00	-2.48
$a_\mu \times 10^{11}$	8.51	3.45	7.22	4.70
$a_\mu^* \times 10^{11}$	3.99	0.93	4.38	1.05
$a_\mu^{**} \times 10^{11}$	0.79	0.28	0.91	0.26
$a_\mu^{***} \times 10^{11}$	0.38	0.14	0.38	0.14
$a_\mu^{****} \times 10^{11}$	0.26	0.1	0.24	0.07
$\check{A}^8(0,0)$	17.74	11.63	17.99	8.95
$\check{A}^0(0,0)$	11.69	-17.75	8.97	-18.00
$\check{\theta}_A$	56.61°	-33.2°	63.515°	-26.4°
$\check{A}(0,0)$	4.89	-3.71	4.17	-4.04
$\check{a}_\mu \times 10^{11}$	13.97	6.95	10.42	8.43
$\check{a}_\mu^* \times 10^{11}$	2.14	0.50	2.61	0.61
$\check{a}_\mu^{**} \times 10^{11}$	0.95	0.30	1.11	0.27
$\check{a}_\mu^{***} \times 10^{11}$	0.41	0.15	0.39	0.15
$\check{a}_\mu^{****} \times 10^{11}$	0.24	0.1	0.23	0.07

TABLE III. Results for the isoscalar axial-vector sector, with gluon condensate parameter Ξ_0 , for the two choices g_5 (OPE fit) and g_5 (F_ρ -fit). Quantities marked by $\check{}$ correspond to the CS' model (Ω_5 without extension by the scalar fields in the superconnection); $\theta_A \equiv \arctan(A^8(0,0)/A^0(0,0))$ for both f_1 and f_1' , and $A(0,0) = \text{tr}(t^a Q^2)A^a(0,0) = [A^8(0,0) + \sqrt{8}A^0(0,0)]/6\sqrt{3}$. All dimensionful quantities are given in units of (powers of) GeV.

of [31] the amplitude for this process can be written as

$$\mathcal{M} = e^4(\varepsilon_\mu \bar{u} \gamma^\mu \gamma^5 v) \frac{N_c}{4\pi^2} \left\{ \int \frac{d^4 k}{(2\pi)^4} \frac{A_{12} + A_{21}}{k^2} + \frac{1}{2} \int \frac{d^4 k}{(2\pi)^4} \left(\frac{A_{12}}{q_2^2} + \frac{A_{21}}{q_1^2} \right) \right\} =: e^4(\varepsilon_\mu \bar{u} \gamma^\mu \gamma^5 v) \bar{\mathcal{M}}, \quad (54)$$

where $A_{12} = A(-q_1^2, -q_2^2)$, $A_{21} = A(-q_2^2, -q_1^2)$ and it is understood that $q_1 = p_1 - k$, $q_2 = p_2 + k$, where p_i are the momenta of the fermions. The vector ε_μ describes the polarization of the axial vector meson and the Dirac spinors \bar{u}, v describe the spins of the electron and the positron. The mass of the electron which appears in $p_i^2 = m_e^2$ can be neglected and we set it to zero in the following analysis. In the decay rate, which can be compared to the experiment, one averages over the initial polarization

of the axial vector meson and adds the probabilities of the different final spins of the electron and positron.

The direct numerical evaluation of the integral appearing in $\bar{\mathcal{M}}$ is challenging with our form for the transition form factors so we use a decomposition of the axial TFF in terms of vector meson modes

$$A(-q_1^2, -q_2^2) = \sum_{\alpha, \beta} M_{\alpha\beta} \frac{1}{q_1^2 - m_\alpha^2 + i\varepsilon} \frac{1}{q_2^2 - m_\beta^2 + i\varepsilon}, \quad (55)$$

with an asymmetric matrix $M_{\alpha\beta}$ defined in (D7) and the sum running over the infinite tower of vector mesons with masses m_α . In the numerical evaluation (see App. D for more details), it is sufficient to let α, β run over the first 60 vector meson modes, modes beyond that can be safely neglected. The decay rate is calculated by

$$\Gamma_{e^+e^-} = \frac{64\pi^3 \alpha^4}{3} m_A |\bar{\mathcal{M}}|^2 \quad (56)$$

and the branching ratio is obtained by dividing by the total experimental decay rate of the axial vector meson, which read $\Gamma = 23.0$ MeV for f_1 and $\Gamma = 56.7$ MeV for f_1' [55]. The results are collected in table IV.

VI. NUMERICAL RESULTS

Fixing the parameters of our model as described in Sec. IV A, the numerical results for meson masses, decay constants, two-photon couplings as well as the resulting a_μ contributions are listed in Table I for pions and a_1 mesons and their first few excited modes. In Table II the same is done for $\eta^{(\prime)}$ pseudoscalar mesons, where G/η'' refers to the mode resulting from the pseudoscalar glueball mixing with η mesons, and in Table III for $f_1^{(\prime)}$ axial-vector mesons, together with a break-up in octet and scalar contributions of decay constants and two-photon couplings. We give numerical results for both the fully scalar-extended CS term (CS'') and the partially scalar-extended one (CS'), marking results for the latter with a breve symbol ($\check{}$). The correspondingly detailed results for the KS model are not reproduced here; for those we refer the reader to [25] and list the final results for the a_μ contribution only in the summary table V.

A. Ground-state pseudoscalars

In the pseudoscalar sector, the achieved agreement with the experimental data was remarkably good in the KS model (v1), at the few-percent level, including the two-photon couplings $F(0,0)$. This is still the case in the CS'' and CS' models, except for $F_{\eta'}(0,0)$, where larger deviations occur, with CS'' underestimating and CS' overestimating $\eta' \rightarrow \gamma\gamma$.

	$\Xi_0 = 0.0158$ $g_5^2 = (2\pi)^2$			$\Xi_0 = 0.0177$ $g_5^2 = 0.894(2\pi)^2$		
	a_1	f_1	f'_1	a_1	f_1	f'_1
m^{exp}	1.23(4)	1.2818(5)	1.4285(14)	1.23(4)	1.2818(5)	1.4285(14)
$m (= \check{m})$	1.429	1.503	1.625	1.371	1.463	1.583
$ A(0,0) $ (L3 exp.)		3.5(4)	2.6(4)		3.5(4)	2.6(4)
$ \mathcal{F}_s(0,0) $ (L3 exp.)		0.88(10)	0.8(1)		0.88(10)	0.8(1)
$\mathcal{F}_s(0,0)$	0.695	1.078[0.01+1.06]	-0.82[-0.35-0.47]	0.658	0.97[-0.01+0.98]	-0.94[-0.33-0.61]
$\check{\mathcal{F}}_s(0,0)$	1.096	1.67[-0.02+1.69]	-1.49[-0.71-0.77]	0.953	1.35[-0.08+1.43]	-1.53 [-0.63-0.90]
Λ_D (L3 exp.)		1.04(8)	0.926(80)		1.04(8)	0.926(80)
Λ	1.045	1.043	1.051	1.035	1.033	1.041
$\check{\Lambda}$	1.009	1.007	1.006	1.006	1.005	1.005
$B_{e^+e^-} \times 10^9$ (SND exp.)		$5.1^{+3.7}_{-2.7}$			$5.1^{+3.7}_{-2.7}$	
$B_{e^+e^-} \times 10^9$		2.48	0.55		2.0	0.76
$\check{B}_{e^+e^-} \times 10^9$		4.74	1.54		3.25	1.79

TABLE IV. Experimental data on f_1 and f'_1 compared with the hQCD predictions in the CS'' model, and also the CS' model (marked by a breve sign $\check{}$). The equivalent photon rates measured by the L3 collaboration [53, 54] are expressed in terms of $|A(0,0)|$ as listed in Table III and also in terms of the parameter used in [56], $\mathcal{F}_s(0,0) \equiv 3m_A^2 A(0,0)/(2\pi^2)$, where for f_1, f'_1 the result is also written as a sum of the $I = 0$ singlet and the $I = 1$ contribution. The parameter Λ_D in the dipole fit of the singly virtual TFF corresponds to Λ in (53). The branching ratio for $f_1 \rightarrow e^+e^-$ has been measured by the SND collaboration [57].

The decay constants and their mixing in the η - η' sector as listed in Table II require a two-angle scheme as introduced in [58, 59]:

$$\theta_8 = \arctan(f_{\eta'}^8/f_{\eta}^8), \quad \theta_0 = -\arctan(f_{\eta}^0/f_{\eta'}^0). \quad (57)$$

Comparing with the lattice results of [60], the results of the KS model (v1) agreed very well with the f^8 scale and reasonably with θ_8 , with somewhat larger deviations for the f^0 scale and θ_0 . The CS'' and CS' models are similar, with a little larger deviation in the octet contributions, but with a noticeable improvement in the f^0 scale, which is now within the range of the (in this case renormalization-scale dependent) lattice result, and some improvement in θ_0 . Ref. [60] also determined the gluonic contribution f_G (corresponding to $\sqrt{N_f}/2a$ in [60]), with a scale dependent ratio $a_{\eta'}/a_{\eta} \equiv f_{G,\eta'}/f_{G,\eta}$ between 2 and 2.5. While the KS result of about 2.6 is somewhat above this range, the CS'' and the CS' model give 2.3, well within. Hence, some features that are clearly associated with the $U(1)_A$ anomaly are more successfully reproduced in the scalar-extended CS models.

B. Ground-state axials

Recently, in [52], a prediction for the singly virtual TFF of the a_1 meson was obtained in the dispersive approach, with

$$\mathcal{F}_s^{a_1, \text{disp.}}(0,0) = 0.76(10). \quad (58)$$

In this case, the CS'' model is at the lower end of this prediction, while the CS' model is 2-3 standard deviations

higher. A somewhat different picture arises if one compares the dimensionful parameter $A^3(0,0)$, because the holographic results for m_A differs from the experimentally observed mass. The prediction of [52] then reads (with slightly reduced relative errors [Peter Stoffer, private communication])

$$A^3(0,0)^{\text{disp.}} = 19.8(1.8) \text{ GeV}^{-2} \quad (59)$$

in terms of the values $A^3 = 6A$ listed in Table I, which are in complete agreement in the CS' case, whereas the CS'' results are now 2-3 standard deviations too low. With regard to $A_{a_1}^3(0,0)$, the best match is, in fact, provided by the KS(F_ρ -fit) model with 19.46 GeV^{-2} . (Note that in the $a = 3$ sector, where the $U(1)_A$ anomaly plays no role, the CS' model is equivalent to the KS model except for slightly different IR boundary conditions.)

In the $a = 8,0$ sector, the CS models provide a somewhat better motivated implementation of the $U(1)_A$ anomaly. While the photon coupling $F_{\eta'}(0,0)$ happens to compare less favorably with the experimental data in these models than the KS model, in the axial-vector sector, the fully scalar-extended CS'' model turns out to give a fairly good match of the experimentally observed equivalent photon rates of f_1 and f'_1 mesons. In contrast to the KS model, the dimensionless ratio $\tilde{\Gamma}_{\gamma\gamma}/m_A$, which is determined by the dimensionless value $\mathcal{F}_s(0,0) \equiv 3m_A^2 A(0,0)/(2\pi^2)$, is only slightly overestimated by the CS'' result, see Table IV. Comparing instead the dimensionful parameter $|A(0,0)|$, the CS'' result is even below the experimental value. On the other hand, the CS' result overestimates both.

In both, the CS'' and the CS' model, the ratio of the amplitude for f_1 over that for f'_1 is larger than 1, in agree-

ment with experiment [53, 54], while this was smaller than 1 in the KS model. This implies that the octet-singlet mixing inferred from experimental data is in the right ballpark. The mixing angle, defined through $A(0,0)$ according to

$$\theta_A \equiv \arctan(A^8(0,0)/A^0(0,0)) \quad (60)$$

and listed in Table III, corresponds to [25] $\theta_A^{\text{exp.}} = 56(5)^\circ$ for f_1 .⁷ The scalar-extended models are much closer to this range than the KS model (v1), which gave $\theta_A \sim 80^\circ$.

C. Transition form factors and a_μ contributions

In Fig. 1, the singly virtual TFFs of the pseudoscalar mesons are compared with compiled data. Here we find for CS'' an excess in particular for π^0 and η , which is associated with the fact that the BL limit turns out to be approached from above. This feature disappears in the CS' model (included by dashed lines). The same behavior shows up in the doubly virtual pion TFF (Fig. 2). Correspondingly the contributions to a_μ are also excessive in the CS'' model, and no longer compatible with the WP2020 estimate as displayed in the summary table V.

In Fig. 3, the shape of the normalized singly virtual TFF of the a_1 meson and also the absolute magnitude of $A^3(Q^2, 0)$ as obtained in the dispersive approach of [52] is compared to the results of the CS'', CS', and KS models. The KS model considered by us in Ref. [25], which in the $a = 3$ sector is identical with the HW1m model of [24] and differs from the CS' model only with respect to boundary conditions (HW3 instead of HW1), turns out to be closest to the dispersive result, which at large Q^2 is due to the fact the HW1 result has a result for the a_1 decay constant that agrees best with the result for the decay constant $F_{a_1}/m_A = 168(7)$ MeV from light-cone sum rules [62] used in [52] to constrain the asymptotic behavior. In fact, in the comparison with the unnormalized $A^3(Q^2, 0)$ (lower panel of Fig. 3), the KS (F_ρ -fit) result is completely within the narrow error band of the dispersive result, for all values of Q^2 .

In Fig. 4, the shape of the singly virtual TFF of f_1 mesons as obtained by a dipole fit of the L3 data [53, 54] is compared with the CS'' and CS' results, showing a good agreement with regard to the slope at small virtualities, but a slower decay at larger ones. Here the KS results are not included in the comparison, because the f_1/f'_1 mixing is too far from the experimental situation.

The doubly virtual TFFs of the axial-vector mesons also determine the branching ratio of e^+e^- decays (see

Fig. 5). The results obtained for the CS'' and CS' models listed in Table IV are fully compatible with the experimental results for $f_1 \rightarrow e^+e^-$ obtained by the SND collaboration in Ref. [57]. The CS'' result is also compatible with the results of the phenomenological study of Ref. [31, 56] (in particular in the fit with better χ^2 obtained by leaving out $f_1 \rightarrow \phi\gamma$ data).

Considering the contribution of the ground-state axial-vector mesons to a_μ , the CS'' model, which provides a rather good fit of equivalent photon rates and mixing angles for f_1 and f'_1 , yields $a_\mu^{a_1+f_1+f'_1} = 16.9 \times 10^{-11}$, incidentally for both the OPE fit and the F_ρ -fit of g_5 . This is significantly lower than the KS (F_ρ -fit) value of 25.0×10^{-11} but still way above the WP2020 value of $6(6) \times 10^{-11}$. Since the squared masses of the ground-state axials are all overestimated in the considered models, larger values would be obtained by manually correcting the masses to their experimental values. In the CS'' (F_ρ -fit), where the ground-state axials have the best match with the L3 data, such an extrapolation would give

$$a_{\mu, \text{CS''}}^{a_1+f_1+f'_1 \text{ extrapol.}} = 20.8 [5.99 + 9.15 + 5.66] \times 10^{-11}. \quad (61)$$

(In [20], using chiral HW models, we had obtained $a_\mu^{a_1+f_1+f'_1} = 17.4(4.0) \times 10^{-11}$ by manually adjusting rates and masses to experimental values; Ref. [18] estimated this contribution as 18.38×10^{-11} ; the recent Dyson-Schwinger analysis of Ref. [63] obtained $19.4(2.1) \times 10^{-11}$.)

However, the reduction of the contribution from the ground-state axial-vector mesons in the CS'' model compared to the KS model is accompanied by a significant increase of the contribution from the tower⁸ of excited axial-vector mesons, see Table V. The total contribution from axial-vector mesons is only about 10% below that in the KS (F_ρ -fit)-model. Including also the contribution from excited pseudoscalars, there is even a net increase.

As already discussed in [24], the two-photon coupling of the first excited pion is much larger than the experimental bound on $\pi(1300)$ (according to [9], $|F_{\pi(1300)\gamma\gamma}| < 0.0544(71)\text{GeV}^{-1}$), and a similar discrepancy occurs for η'' if this is identified with $\eta(1475)$ for which the results from the L3 experiment [54] imply $F(0,0) = 0.041(6)\text{GeV}^{-1}$. In [24] we interpreted the much larger values appearing for π^* and G/η'' in Tables I and II as reflecting the collective effect of the much denser spectrum of excited pseudoscalars in real QCD compared to the HW models. Since these contributions turn out to be rather model dependent, they should perhaps be better viewed

⁷ The conventional definition of the mixing angle θ_A in terms of the dimensionless ratio $\tilde{\Gamma}_{\gamma\gamma}/m_A$ or \mathcal{F}_s would give $\theta_A^{\text{exp.}} = 62(5)^\circ$. The hQCD result corresponds instead to a definition in terms of the ratio $\tilde{\Gamma}_{\gamma\gamma}/m_A^5$. Also the analysis of Ref. [61] suggests a dependence of $\tilde{\Gamma}_{\gamma\gamma}/m_A$ on m_A , albeit with a different power.

⁸ The sum over excited axials is carried out using the extrapolation described in [25]. Comparing with an approximate numerical evaluation using the axial vector bulk-to-bulk propagator we estimate the possible numerical error in the complete sum over the axial-vector towers as $+0.6$ and -0.2×10^{-11} .

as variable parts of the effect of the universal LSDC. In fact, the total sum of contributions from the towers of axials and pseudoscalars shows remarkable stability across the models considered here.

VII. DISCUSSION AND CONCLUSIONS

In Ref. [25] we have considered the KS model [26], where only the standard 5-form part Ω_5 (and this without scalars) is included in the Chern-Simons action and where the $U(1)_A$ anomaly is incorporated by a slightly simpler addition to the 5-dimensional Lagrangian. Allowing for a gluon condensate as one further parameter, this gave an excellent match of experimental constraints on the pseudoscalar sector, with masses and photon couplings agreeing with data at the percent level. Evaluating the pseudoscalar TFFs, we found good agreement with phenomenological and lattice results when using a reduced 5-dimensional gauge coupling (F_ρ -fit) reflecting gluonic corrections, and the resulting HLBL contributions to a_μ turned out to agree perfectly with the WP2020 estimates. (However, there is less good agreement with the more recent evaluation of Ref. [64] which has smaller contributions from η and η' , see Table V.)

In the best-fitting $KS(F_\rho\text{-fit})$ model, the axial-vector sector, which is responsible for satisfying the longitudinal SDC, was found to contribute $a_\mu^{\text{AV+LSDC}} = 30.5 \times 10^{-11}$ (32.1×10^{-11} when excited pseudoscalars are included), slightly larger but consistent with the WP2020 estimate of $21(16) \times 10^{-11}$, see Table V. However, in the KS model, the axial vector mesons in the $a = 8, 0$ sector are found to have stronger deviations from experimental data: the masses of f_1 and f'_1 mesons are 10% and 28% too high, respectively, their mixing angle deviates strongly from experimental findings, and the equivalent photon rates are too high. On the other hand, the combined contribution of f_1 and f'_1 to a_μ should be fairly independent of their mixing, and the excesses in masses and photon couplings should partially compensate in a_μ .

This points to the need for further refinements, and the improved hQCD models developed in Ref. [29, 32–34, 48, 49] present several options. However, it is certainly interesting to have alternative hQCD models which also include flavor-symmetry breaking by quark masses and the $U(1)_A$ anomaly, while keeping the number of free parameters at a minimum. This is indeed the case with the HW models involving a scalar-extended Chern-Simons term, and we have considered these extensions in two versions, called CS'' and CS' in Table V, where CS'' refers to the case where a scalar potential appears in both terms in (3), while in CS' this is the case only for the first. (Without any scalar extension, the model is still different from the KS model, but the results are then rather similar.)

Remarkably, both versions improve the results in the axial-vector sector with regard to masses, mixing, and photon couplings. The masses of the ground-state axial-

vector mesons are still too high, but only up to +17%; the f_1 - f'_1 mixing angle is close to the experimentally observed ball-park; and the values of $\mathcal{F}_s(0, 0)$ determining the equivalent photon rates are almost within the experimental error band for the CS'' model (with either full or reduced g_5). The CS' model overestimates $\mathcal{F}_s(0, 0)$ similarly to the KS model. Since the masses are too high, this should in fact tend to underestimate the contributions of the ground-state axial-vector mesons in the CS'' model.

However, the pseudoscalar sector, where the corresponding parameters are nearly perfect in the KS model, shows larger deviations in the photon coupling of η' mesons, up to -20% in the CS'' model and up to +26% in the CS' one, see Table II. While the CS' model has pseudoscalar TFFs that agree similarly well with data than the KS model, they are strongly overestimated at nonzero virtualities in the CS'' model, approaching the BL limit from above. In the CS'' model, the π^0 contribution is thus much higher than the WP2020 estimate, and also the excited pseudoscalars turn out to contribute significantly more than in the other models.

Nevertheless, in the CS'' model, the sum of pseudoscalar and axial-vector contributions is almost unchanged compared to the KS model.

Since the $KS(F_\rho\text{-fit})$ model with reduced g_5 provides the best match in the experimentally more constrained pseudoscalar sector, we consider it still the preferred model for making predictions for both pseudoscalar and axial-vector contributions as well as associated LSDC effects in a_μ , where the combined contribution from f_1 and f'_1 should be relatively insensitive to their precise octet-singlet mixing. The $KS(F_\rho\text{-fit})$ model appears also validated by a comparison with the recent dispersive results for the singly virtual a_1 TFF (see Fig. 3). We therefore propose to take the range of results added by the CS'' and CS' models as systematic error estimates within the class of HW hQCD models which include flavor-symmetry violating effects⁹. For the complete tower of axial-vector mesons whose longitudinal parts saturate the MV-SDC, we thus obtain for the a_μ contributions with F_ρ -fitted coupling (31)

$$a_\mu^{\text{AV+LSDC}} = 31.1^{+2.9}_{-4.1} \times 10^{-11}. \quad (62)$$

[The recent estimate obtained in [63] in a DSE/BSE calculation of $27.5(3.2) \times 10^{-11}$ happens to be fully compatible with this hQCD result.¹⁰ This is also the case for the simple Regge-like model for axial vector mesons constructed in Ref. [18], which produced an estimate of 31.41×10^{-11} .]

⁹ In the soft-wall model of [65] that also includes the strange quark mass and the $U(1)_A$ anomaly along the lines of [29], only the pseudoscalar contributions were evaluated; the axial-vector contributions obtained in [47] were obtained in a flavor-symmetric model.

¹⁰ Note, however, that the approximations used therein neglect the $U(1)_A$ anomaly, which also affects the axial-vector sector in the hQCD models.

$a_\mu \times 10^{11}$	KS(OPE fit)	KS(F_ρ -fit)	CS''(OPE fit)	CS''(F_ρ -fit)	CS'(OPE fit)	CS'(F_ρ -fit)	WP2020	Ref. [64]
π^0	66.1	63.4	73.3	68.8	66.6	64.3	$62.6^{+3.0}_{-2.5}$	
η	19.3	17.6	19.4	17.2	18.7	17.7	16.3(1.4)	14.7(9)
η'	16.9	14.9	14.9	12.2	21.4	20.1	14.5(1.9)	13.5(7)
G/η''	0.2	0.2	2.0	2.6	0.8	0.9		
\sum_{PS^*}	1.6	1.4	3.5	3.2	1.2	0.8		
$\pi^0 + \eta + \eta'$	102.3	95.9	107.6	98.2	106.7	102.1	93.8(4.0)	$91.2^{+2.9}_{-2.4}$
PS poles total	104	97.5	113	104	109	104		
a_1	7.8	7.1	4.9	4.9	8.2	7.6		
$f_1 + f_1'$	20.0	17.9	12.0	12.0	20.9	18.9		
$\sum_{a_1^*}$	2.5 [†]	2.6 [†]	2.5	2.3	1.7	1.7		
$\sum_{f_1^{(\prime)*}}$	4.0 [†]	3.5 [†]	7.4	7.9	5.3	5.9		
AV+LSDC total	34.3	31.1	26.7	27.0	36.1	34.0		
AV+P*+LSDC total	36.0	32.7	32.2	32.8	38.2	35.7	21(16)	
total	138	129	140	131	145	138	115(16.5)	

TABLE V. Summary of the results for the different contributions to a_μ in comparison with the White Paper [4] values and with the new results on $a_\mu^{\eta, \eta'}$ from [64]. KS refers to the Katz-Schwartz model used by us in Ref. [25], CS'' is the fully scalar-extended case, and CS' is without scalars in Ω_5 ; the two choices (30) and (31) for g_5 are denoted by (OPE fit) and (F_ρ -fit), respectively. The numbers marked by a dagger have been obtained using the full bulk-to-bulk axial vector propagator; they supersede the somewhat lower estimates obtained in Ref. [25] from extrapolating sums over the first few excited modes.

Adding the excited pseudoscalars (including G/η''), which also contribute to the part of the HLBL tensor that is involved in the MV-SDC, the KS value is somewhat higher and the downward variation is reduced to zero,¹¹

$$a_\mu^{\text{AV+P*+LSDC}} = 32.7^{+3.0}_{-0.0} \times 10^{-11}. \quad (63)$$

It is presumably this latter result which is to be compared with the WP2020 estimate of $21(16) \times 10^{-11}$ for the sum of axial-vector and SDC contributions, as the estimate for the latter involved a model for excited pseudoscalars. It should be noted, however, that the hQCD results only capture fully the LSDC; the SDC for $\bar{1}_1$ in the symmetric high-momentum limit has the correct Q^2 behavior, but reaches only 81% of the OPE value.¹²

We would like to recall that the HW hQCD models we have studied are comparatively minimal models. They have just enough free parameters to match f_π , m_ρ , and $N_f = 2 + 1$ quark masses. The coupling g_5 , which is usually fixed by the leading-order OPE result for the vector correlator, has been allowed to be replaced by a fit of F_ρ , which happens to reproduce typical NLO corrections in the vector correlator as well as in TFFs.

The only extra freedom introduced was a nonzero value for the gluon condensate that turned out to permit accurate fits of η and η' masses. The three models KS, CS'', and CS' differ in their implementation of the $U(1)_A$ anomaly and whether the bi-fundamental field is included in the Chern-Simons terms. The simpler KS model led to the best fit in the pseudoscalar sector, while the scalar-extended CS'' achieved the best fit to f_1 and f_1' mesons, however at the expense of poor agreement of the π^0 TFF with data. However, for $a_\mu^{\text{AV+P*+LSDC}}$ the CS'' model yields almost the same result as the KS model, which we take as a validation of the results obtained in the latter.

Nevertheless, it would be interesting to see how stable this result is upon further improvements of the hQCD model. In [65], it was found that a simple soft-wall model with a dilaton quadratic in z permits a good fit of masses and two-photon couplings of pseudoscalars, but strongly overestimates the π^0 TFF, which as in the CS'' model approaches the BL limit from above. In fact, in other applications, it was noticed before [67] that soft-wall models are phenomenologically less successful than HW models, and this is also the case with regard to the HVP contribution to a_μ [43]. A more promising, but also more difficult alternative is provided by the improved hQCD models in the Veneziano limit of Ref. [29, 32–34, 48, 49], which permit the implementation of a running coupling and which indeed combine features of hard-wall models through an effective cutoff of the 5-dimensional space-time with (asymptotically) linear Regge trajectories as in soft-wall models. The results obtained in the present study suggest that a combined high-precision fit of low-

¹¹ In [24], also the effect of a larger reduction of g_5^2 by 15% instead of 10% was considered, which diminishes the axial-vector contributions by an additional 3%. Including that would give a downward variation of about 1×10^{-11} .

¹² As shown recently in Ref. [66], this gap can be filled by tensor meson contributions without modifying the MV-SDC.

energy data in the pseudoscalar and axial-vector sector seems possible, which would improve further the significance of hQCD results for the HLBL contribution to the muon anomalous magnetic moment.

After this work has been finished, a dispersive analysis of axial-vector contributions to a_μ has appeared in Refs. [68, 69] which also finds significantly larger contributions from axial vector mesons than assumed in the White Paper of 2020 [4]. In Appendix E these results are compared with the holographic ones with regard to different energy regions of the HLBL amplitude, and the contributions associated with the axial sector turn out to be quite comparable, in particular with our “best-guess” $KS(F_\rho\text{-fit})$ model.¹³

ACKNOWLEDGMENTS

We would like to thank Martin Hoferichter, Elias Kiritsis, Pablo Sanchez Puertas, Peter Stoffer, and Marvin Zanke for helpful discussions. We are particularly grateful to Peter Stoffer for providing the detailed results for the a_1 TFF in the dispersive analysis of Ref. [52]. This work has been supported by the Austrian Science Fund FWF, project no. PAT 7221623.

Appendix A: Relation between T and X

In this appendix we derive the multiplicative factor relating the tachyon T and the HW field X^\dagger . We first list the relevant DBI action and definitions of [29] with $2\pi\alpha'$ reinstated and with T having mass dimension 1:

$$S_{DBI} = -T_p \int d^{p+1}x e^{-\phi} \text{SymTr} \left(V_t(T^\dagger T) \sqrt{-\det B_L} + V_t(TT^\dagger) \sqrt{-\det B_R} \right) \quad (\text{A1})$$

with

$$V_t(TT^\dagger) = e^{-2\pi\alpha' T^\dagger T}, \quad (\text{A2})$$

$$B_{L,MN} = (g + B)_{MN} + 2\pi\alpha' F_{MN}^L + 4\pi\alpha'^2 ((D_M T)^\dagger D_N T + (D_N T)^\dagger D_M T), \quad (\text{A3})$$

$$B_{R,MN} = (g + B)_{MN} + 2\pi\alpha' F_{MN}^R + 4\pi\alpha'^2 (D_M T (D_N T)^\dagger + D_N T (D_M T)^\dagger), \quad (\text{A4})$$

and

$$D_M T = \partial_M T + iT A_M^L - iA_M^R T. \quad (\text{A5})$$

The expression $\sqrt{-\det B_L}$ is mathematically ambiguous since B_L has both spacetime and flavor indices and needs to be properly defined. The determinant should only act on the spacetime indices. We first pull out a factor of the determinant of the metric to arrive at

$$\sqrt{g} \sqrt{\det(1 + C)}, \quad (\text{A6})$$

with $C_L = B_N^M + 2\pi\alpha' (F_L)^M_N + 4\pi\alpha'^2 (D^M T^\dagger D_N T + D^N T^\dagger D_M T)$ and similar for C_R . In the following, we will ignore the Kalb-Ramond field B . We take the second factor to mean

$$\sqrt{\det(1 + C)} = \exp \left(\frac{1}{2} \text{tr}_L \sum_{n=1} \frac{(-1)^{n+1} C^n}{n} \right). \quad (\text{A7})$$

Here C^n means that one should contract spacetime and flavor indices and the trace is only over the spacetime indices. We don't claim this is the correct full DBI action, we just use this prescription to expand in the lowest orders of α' . Performing this expansion, one arrives at¹⁴

$$S_{DBI} = -\frac{1}{4g_5^2} \int_{AdS_5} \sqrt{g} \text{tr} \left((F_L)_{MN} (F_L)^{MN} + (F_R)_{MN} (F_R)^{MN} \right) + \frac{4\alpha'}{g_5^2 2\pi\alpha'} \int_{AdS_5} \sqrt{g} \text{tr} (D_M T D_N T^\dagger g^{MN} + \frac{1}{2\alpha'} T T^\dagger). \quad (\text{A8})$$

The coupling constant is given in terms of the string theory parameters as $g_5^{-2} = (2\pi\alpha')^2 T_p e^{-\phi_0} V(K)$, where $V(K)$ is the volume of possible compact directions K that have been integrated out. Upon taking $1/(2\alpha') = 3/R^2$, with R the AdS radius we can redefine the tachyon

$$X = \frac{1}{g_5} \sqrt{\frac{2}{\pi}} T^\dagger \quad (\text{A9})$$

to arrive at the usual HW action for X . The adjoint arises because of the definition (A5) compared to our usual conventions for the covariant derivative of the scalar X .

Appendix B: Quadratic terms and radiative couplings in the Chern-Simons term

In this appendix, we derive more explicit formulas for Ω_1 and Ω_5 , at least when considering pseudoscalar fluctuations of the bi-fundamental scalar T only. Many relevant formulas were already derived in [29], but only in the special case of a tachyon background proportional to the identity. As we want to consider a differing strange quark

¹³ Ref. [69] also includes contributions from tensor mesons, where a full dispersive treatment is not yet available. Using a simple quark model much larger contributions than previously obtained [70] have been found. Tensor meson contributions have now also been worked out in HW hQCD models, which turn out to be of comparable magnitude but different sign [66, 71].

¹⁴ The definitions from before are in the mostly + convention, while the following formula has converted it already to mostly - as in the main text.

mass, we must generalize these formulas. The exponential in (1) is defined by using the series expansion for the exponential, one crucial difference is that in the matrix multiplication there are extra signs depending on the form degrees of the components, we refer the reader to [29] for the relevant definitions. We start with Ω_1 , which can be extracted from the 2-form part of $\text{Str exp } i2\pi\alpha'\mathcal{F}$. We split \mathcal{F} into background contributions and terms linear in fluctuations. In accordance with (4) and (8) we parameterize fluctuations of the tachyon as $T = e^{-i\eta T_0} e^{-i\eta}$.

The background contributions split into terms of different form-degree

$$i\mathcal{F}_{bg} = \begin{pmatrix} -T_0^2 & \\ & -T_0^2 \end{pmatrix} + \begin{pmatrix} & dT_0 \\ dT_0 & \end{pmatrix}. \quad (\text{B1})$$

The 2 form part of $\text{Str exp } i2\pi\alpha'\mathcal{F}$ splits into a term containing no dT_0 and a part containing one dT_0 . After using the definitions for the multiplication of supermatrices and the supertrace these read

$$i2\pi\alpha' \text{tr} e^{-2\pi\alpha'T_0^2} d(A_L - A_R) \quad (\text{B2})$$

and

$$i2\pi\alpha' \text{tr} de^{-2\pi\alpha'T_0^2} (-2d\eta + (A_L - A_R)). \quad (\text{B3})$$

This immediately leads to an expression for Ω_1 :

$$\Omega_1 = 4\pi\alpha' \text{tr}(e^{-2\pi\alpha'T_0^2} A + \eta de^{-2\pi\alpha'T_0^2}). \quad (\text{B4})$$

As explained in the main text, any other choice of Ω_1 (which differs by an exact term) can be absorbed in a redefinition of the scalar a .

For the computation of Ω_5 , we need to restrict to the 6-form part of $\text{Str exp } i2\pi\alpha'\mathcal{F}$. One way of computing Ω is using an explicit formula which reads

$$\Omega(\mathcal{A}) = 2\pi\alpha' i \int_0^1 \text{Str exp}(2\pi\alpha' i \mathcal{F}_t) \partial_t A_t, \quad (\text{B5})$$

where A_t is a one parameter family of connections with $\mathcal{A}_1 = \mathcal{A}$ and \mathcal{A}_0 having vanishing curvature.

Since we will only use this part of the action to compute transition functions for mesons which are described by modes that sit in the diagonal parts of the flavor matrices, we can take the fluctuations η and the gauge fields A_L, A_R to commute with the background T_0 . For the one-parameter family of superconnections we take

$$i\mathcal{A}_t = t \begin{pmatrix} iA_L & \\ & iA_R \end{pmatrix} + \begin{pmatrix} & dT^\dagger \\ dT & \end{pmatrix}. \quad (\text{B6})$$

The superconnection at $t = 0$ does not have zero curvature in general, but it does not contain any AVV or ηVV terms, which are relevant for radiative decays. Hence the curvature at $t = 0$ does not contribute to the processes we consider.

The ηVV terms we get from (B5) read

$$i(2\pi\alpha')^3 \text{tr}(de^{-2\pi\alpha'T_0^2} d\eta dV). \quad (\text{B7})$$

The two AVV contributions read

$$-i(2\pi\alpha')^3 \frac{1}{6} \text{tr} e^{-2\pi\alpha'T_0^2} (A_L dA_L^2 - A_R dA_R^2) \quad (\text{B8})$$

and

$$-i(2\pi\alpha')^3 \frac{2}{6} \text{tr} de^{-2\pi\alpha'T_0^2} dV (A_L - A_R). \quad (\text{B9})$$

In the above formulas we eventually replace the tachyon background with (4) (we also have $A_{L/R} = V \pm A$). We stress again that the above formulas are only valid for the meson modes sitting in the diagonal part of the flavor matrices. We note that we have performed no partial integrations to arrive at the above formulas. One may calculate the TFFs for pseudoscalar and axial vector mesons by standard procedures from the above expressions.

In the term $(da - \tilde{\Omega}_1) * (da - \tilde{\Omega}_1)$ one might also suspect radiative couplings (for example of the form aVV) when considering higher order fluctuations in $\tilde{\Omega}_1$. Using (B5), it is easy to see that no such couplings can be produced (one has to use the 1-parameter family $\mathcal{A}_t = tA$).

Characteristic for this Chern-Simons term are the $e^{-2\pi\alpha'T_0^2}$ factors. They also provide at least a qualitative solution to a potential problem in the study of glueballs decaying into two photons. When considering such processes in models with the non-scalar extended Chern-Simons term one gets a factor of $\text{tr}(\mathcal{Q}^2)$ from couplings of flavor-neutral fields to the flavor fields. This could be, for example, a coupling of the Kalb-Ramond field B , some RR field C , or the metric through the \hat{A} -genus to the flavor gauge fields. The value of $\text{tr}(\mathcal{Q}^2)$ depends rather strongly on the number of flavors of quarks one considers, while in real QCD the decay into two photons should not be sensitive to whether there exists a very heavy quark or not. The scalar extended CS term resolves this qualitatively since for a very heavy quark $e^{-2\pi\alpha'T_0^2}$ goes to zero very quickly and only contributes at very small z , which roughly translates to very high energies.

Appendix C: Scalar TFFs

For scalars, the amplitude into two photons can be written as

$$\mathcal{M}^{\mu\nu} = T_1^{\mu\nu} \mathcal{F}_1 + T_2^{\mu\nu} \mathcal{F}_2 \quad (\text{C1})$$

with

$$\mathcal{F}_1 = -\gamma \frac{8\pi^2\alpha'}{4} \int \frac{dz}{z} \text{tr} \left(\mathcal{Q}^2 S(z) X_0(z) \right) \mathcal{J}(q_1, z) \mathcal{J}(q_2, z), \quad (\text{C2})$$

$$\mathcal{F}_2 = -\gamma \frac{8\pi^2\alpha'}{4} \int \frac{dz}{z} \text{tr} \left(\mathcal{Q}^2 S(z) X_0(z) \right) \frac{\mathcal{J}'(q_1, z)}{q_1^2} \frac{\mathcal{J}'(q_2, z)}{q_2^2}. \quad (\text{C3})$$

This agrees with the results obtained in [72], but there a chiral model was considered, where $X_0(z) \sim z^3$ for $z \rightarrow 0$. Since we work with nonzero quark masses, we have $X_0(z) \sim z$ instead, we get a different asymptotic behavior, namely

$$\mathcal{F}_1 \propto \frac{1}{Q^4} \frac{1}{w^4} \left[3 - 2w^2 + \frac{3}{2w} (1 - w^2) \ln \frac{1 - w}{1 + w} \right] \quad (\text{C4})$$

$$\mathcal{F}_2 \propto \frac{1}{Q^6} \frac{1}{w^4} \left[3 + \frac{1}{2w} (3 - w^2) \ln \frac{1 - w}{1 + w} \right], \quad (\text{C5})$$

whereas [72] obtained $\mathcal{F}_1 \sim Q^{-6}$ and $\mathcal{F}_2 \sim Q^{-8}$, with a different w -dependence.

Generalizing the pQCD calculations of Brodsky and Lepage (BL) for the pseudoscalar TFF, the authors of [22] have obtained instead a result with the even weaker fall-off $\mathcal{F}_1 \sim Q^{-2}$ and $\mathcal{F}_2 \sim Q^{-4}$, where both asymmetry functions are proportional to a function $f^S(w)$ that also appears in the above result in (C4) but not in (C5).

The OPE of the product of two electromagnetic currents in fact contains a scalar contribution of the form

$$\int d^4x e^{iqx} J^\mu(x) J^\nu(0) \sim \frac{2}{q^4} (g^{\mu\nu} q^2 - q^\mu q^\nu) \bar{\psi} \mathcal{Q}^2 m \psi + \dots \quad (\text{C6})$$

which is indeed consistent with the holographic result for nonvanishing quark masses. This is not in contradiction with the BL result of [22] and also the slightly older study of [73], since in the limit of $q_1^\mu \rightarrow -q_2^\mu$ one has $T_2^{\mu\nu} \rightarrow -q^2 T_1^{\mu\nu}$ and the leading $1/q^2$ terms therein cancel at this symmetric point. However, in contrast to the situation for pseudoscalars and axial vector mesons, there is a contradiction between the BL result and the holographic one away from this point, including the symmetric point with $q_1^\mu \rightarrow +q_2^\mu$, which is beyond the applicability of the OPE analysis.

As an aside, we would like to mention that a discrepancy between the BL results of [22] and holographic results for TFFs was also found in the case of tensor mesons [47]. However, in this case, there is in fact a difference between the operators involved: on the holographic side the dual operator to the tensor mesons as introduced in [47] is the (flavor-singlet) full energy-momentum tensor, and not actually the operator underlying the analysis of Ref. [22].

Appendix D: Evaluation of the electron-positron decay amplitude of axial-vector mesons

In the evaluation of the electron-positron decay amplitude we use the decomposition of the axial-vector TFF (55) in terms of vector meson modes with masses m_α . This decomposition can be derived by inserting the decompositions $\mathcal{J}(z, q) = \sum_\alpha \frac{f_\alpha \rho_\alpha(z)}{q^2 - m_\alpha^2 + i\varepsilon}$ and

$$\frac{\partial_z \mathcal{J}(z, q)}{q^2} = \sum_\alpha \frac{1}{m_\alpha^2} \frac{f_\alpha \rho'_\alpha(z)}{q^2 - m_\alpha^2 + i\varepsilon} \quad (\text{D1})$$

into the expression for $A(q_1^2, q_2^2)$. Here the function $\rho_\alpha(z)$ is a vector meson mode obeying

$$\partial_z \left(\frac{\partial_z \rho_\alpha}{z} \right) + \frac{m_\alpha^2 \rho_\alpha}{z} = 0 \quad (\text{D2})$$

with normalization such that $\frac{1}{g_5^2} \int \frac{\rho^2}{z} = 1$. If one just straightforwardly takes the decomposition for $\mathcal{J}(z, q)$, and computes $\frac{\partial_z \mathcal{J}(z, q)}{q^2}$ one will get something different from (D1). The expression that one would obtain in this way would be a sum that diverges at $q^2 = 0$ when truncated at any finite mode number. The expression (D1) is finite at $q^2 = 0$ even when truncating the sum at any finite mode number. To derive (D1), we note that $\lambda := \frac{\partial_z \mathcal{J}(z, q)}{q^2}$ obeys the equation

$$\left(z \left(\frac{\lambda}{z} \right)' \right)' + q^2 \lambda = 0. \quad (\text{D3})$$

To successfully decompose λ we should look for modes of this equation. The new modes $\tilde{\rho}$ will, of course, be proportional to ρ'_α , but they will have a nontrivial prefactor N_α to account for their norm. Using $\tilde{\rho}_\alpha = N_\alpha \rho'_\alpha$, we have

$$1 = \frac{1}{g_5^2} \int \frac{\tilde{\rho}_\alpha^2}{z} = N_\alpha^2 m_\alpha^2, \quad (\text{D4})$$

which implies $N_\alpha = \frac{1}{m_\alpha}$. In order to calculate the inner product between the mode λ and one of these normed modes, we compute

$$(q^2 - m_\alpha^2) \langle \tilde{\rho}_\alpha, \lambda \rangle = (q^2 - m_\alpha^2) \int dz \frac{\tilde{\rho}_\alpha(z) \lambda(z)}{g_5^2 z} \quad (\text{D5})$$

$$= -\frac{1}{g_5^2} \left(\tilde{\rho}_\alpha \left(\frac{\lambda}{z} \right)' - \lambda \left(\frac{\tilde{\rho}_\alpha}{z} \right)' \right) \Big|_{\varepsilon^0} = -\frac{1}{g_5^2} \tilde{\rho}'_\alpha(\varepsilon) = \frac{f_\alpha}{m_\alpha}. \quad (\text{D6})$$

The last equality comes from using the small z asymptotics $\lambda = -z \log z$ and $\tilde{\rho} \sim z$. Combining all these ingredients one arrives at (D1). The expression for $M_{\alpha\beta}$ then reads

$$M_{\alpha\beta} = 2 \frac{f_\alpha}{m_\alpha^2} f_\beta \int dz \rho'_\alpha(z) \rho_\beta(z) W^a \xi^a(z). \quad (\text{D7})$$

After insertion of (55) into (54), one can introduce Feynman parameters u_1, u_2 for each α, β and perform the integral over the loop variable k . In addition, one can integrate out u_2 analytically. The result for the quantity

$\bar{\mathcal{M}}$ in (54) is

$$\begin{aligned} \bar{\mathcal{M}} = & \frac{N_c}{4\pi^2} \frac{-i}{(4\pi)^2} \sum_{\alpha\beta} M_{\alpha\beta} \int_0^1 du_1 \\ & \left\{ -\frac{1}{m_\beta^2} \log [-m_A^2 u_1 (1-u_1) + m_\alpha^2 u_1 - i\varepsilon] \right. \\ & + \frac{1}{m_\beta^2} \log [(m_\beta^2 - m_A^2 u_1)(1-u_1) + m_\alpha^2 u_1 - i\varepsilon] \\ & \left. + \frac{2}{m_\beta^2 - m_A^2 u_1} \log \left[\frac{u_1 m_\alpha^2 + (1-u_1)(m_\beta^2 - m_A^2 u_1) - i\varepsilon}{u_1 m_\alpha^2 - i\varepsilon} \right] \right\}. \end{aligned} \quad (\text{D8})$$

This integral can be performed numerically to high precision, provided the $i\varepsilon$ prescription is properly taken into account. We have crosschecked our numerical results by performing a PV reduction using FeynCalc 9.3.1 [74] and evaluating the standard integrals using LoopTools [75] in Mathematica. Using the PV definitions the integral of the last 3 lines of the previous equation can be expressed as

$$\begin{aligned} & -2C_0(m_A^2, 0, 0, m_\alpha^2, m_\beta^2, 0) \\ & - \frac{B_0(m_A^2, m_\alpha^2, m_\beta^2) - B_0(m_A^2, 0, m_\beta^2)}{m_\alpha^2} \end{aligned} \quad (\text{D9})$$

and directly evaluated using LoopTools.

Appendix E: Comparison with Ref. [69]

For the sake of comparison with the recent study [69] (HSZ) of the subleading contributions to a_μ^{HLBL} from the axial sector, Table VI shows the various contributions from the low-energy (IR) and mixed IR-UV regions of integration, defined by the separation scale $Q_0 = 1.5$, for the KS and CS'' models with the reduced g_5^2 obtained by fitting F_ρ .

This shows a remarkable agreement of the KS(F_ρ -fit) model with the dispersive results for axial-vector contributions in the IR region and only a small deviation in the mixed region; the CS'' model agrees well with regard to the total sum in the IR region, while the distribution over the various contribution is not reproduced.

The mixed region contributions in the HSZ results [69] also include contributions other than from the axial sector, in particular tensor meson contributions, which have been found to be larger than previously estimated. Tensor meson contributions to a_μ have most recently also been evaluated in hQCD for the HW geometry shared by the KS and CS models considered here, resulting in similarly large contributions, but with opposite sign, see Ref. [71].

Ref. [69] also lists longitudinal ($\bar{\Pi}_{1,2}$) and transverse ($\bar{\Pi}_{3-12}$) parts of the various contributions. There the axial vector contributions are 58-59% longitudinal, where

the various axial vector contributions in the hQCD models have a 54-55% longitudinal fraction. Including the excited pseudoscalars, which are purely longitudinal and which are not present in the HSZ result, the overall longitudinal part becomes 59% in the KS(F_ρ -fit) model, equal to the amount in the dispersive result, whereas the CS'' model has 70%.

Region	$a_\mu^{\text{HLBL}} \times 10^{11}$	KS(F_ρ -fit)	CS''(F_ρ -fit)	HSZ[69]
IR	a_1	4.2	2.5	3.8(7)
	$f_1 + f_1'$	8.9	5.9	8.4(1.4)
	AV^*	0.7	1.7	
	PS^*	1.7	4.8	
	eff.poles			2.0
	Sum	15.4	14.8	14.2(1.6)
Mixed	a_1	2.4	1.95	
	$f_1 + f_1'$	7.1	4.75	
	AV^*	1.9	1.7	
	PS^*	-0.04	1.0	
	Sum	11.4	8.4	15.9(1.0)
IR+Mixed Sum		26.8	25.2	30.0(1.9)

TABLE VI. Low-energy (IR) region ($Q_i < Q_0 = 1.5$ GeV for all i) and mixed region contributions compared to the recent evaluation of subleading contributions in the dispersive approach of Ref. [69] (HSZ). In the mixed region, the HSZ result is not exclusively from the axial sector but instead involves OPE results in certain subregions as well as scalar and tensor contributions.

-
- [1] **Muon g-2** Collaboration, D. P. Aguillard et al., *Measurement of the Positive Muon Anomalous Magnetic Moment to 0.20 ppm*, *Phys. Rev. Lett.* **131** (2023), no. 16 161802, [arXiv:2308.06230].
- [2] **Muon g-2** Collaboration, D. P. Aguillard et al., *Detailed report on the measurement of the positive muon anomalous magnetic moment to 0.20 ppm*, *Phys. Rev. D* **110** (2024), no. 3 032009, [arXiv:2402.15410].
- [3] G. Colangelo et al., *Prospects for precise predictions of a_μ in the Standard Model*, arXiv:2203.15810.
- [4] T. Aoyama et al., *The anomalous magnetic moment of the muon in the Standard Model*, *Phys. Rept.* **887** (2020) 1–166, [arXiv:2006.04822].
- [5] K. Melnikov and A. Vainshtein, *Hadronic light-by-light scattering contribution to the muon anomalous magnetic moment revisited*, *Phys. Rev.* **D70** (2004) 113006, [hep-ph/0312226].
- [6] J. Bijnens, N. Hermansson-Truedsson, and A. Rodríguez-Sánchez, *Short-distance constraints for the HLbL contribution to the muon anomalous magnetic moment*, *Phys. Lett. B* **798** (2019) 134994, [arXiv:1908.03331].
- [7] J. Bijnens, N. Hermansson-Truedsson, L. Laub, and A. Rodríguez-Sánchez, *Short-distance HLbL contributions to the muon anomalous magnetic moment beyond perturbation theory*, *JHEP* **10** (2020) 203, [arXiv:2008.13487].
- [8] G. Colangelo, F. Hagelstein, M. Hoferichter, L. Laub, and P. Stoffer, *Short-distance constraints on hadronic light-by-light scattering in the anomalous magnetic moment of the muon*, *Phys. Rev. D* **101** (2020) 051501, [arXiv:1910.11881].
- [9] G. Colangelo, F. Hagelstein, M. Hoferichter, L. Laub, and P. Stoffer, *Longitudinal short-distance constraints for the hadronic light-by-light contribution to $(g-2)_\mu$ with large- N_c Regge models*, *JHEP* **03** (2020) 101, [arXiv:1910.13432].
- [10] J. Lüdtkke and M. Procura, *Effects of longitudinal short-distance constraints on the hadronic light-by-light contribution to the muon $g-2$* , *Eur. Phys. J. C* **80** (2020), no. 12 1108, [arXiv:2006.00007].
- [11] G. Colangelo, F. Hagelstein, M. Hoferichter, L. Laub, and P. Stoffer, *Short-distance constraints for the longitudinal component of the hadronic light-by-light amplitude: an update*, *Eur. Phys. J. C* **81** (2021), no. 8 702, [arXiv:2106.13222].
- [12] M. Knecht, *On some short-distance properties of the fourth-rank hadronic vacuum polarization tensor and the anomalous magnetic moment of the muon*, *JHEP* **08** (2020) 056, [arXiv:2005.09929].
- [13] J. Bijnens, N. Hermansson-Truedsson, L. Laub, and A. Rodríguez-Sánchez, *The two-loop perturbative correction to the $(g-2)_\mu$ HLbL at short distances*, *JHEP* **04** (2021) 240, [arXiv:2101.09169].
- [14] J. Bijnens, N. Hermansson-Truedsson, and A. Rodríguez-Sánchez, *Constraints on the hadronic light-by-light in the Melnikov-Vainshtein regime*, *JHEP* **02** (2023) 167, [arXiv:2211.17183].
- [15] V. Pauk and M. Vanderhaeghen, *Single meson contributions to the muon’s anomalous magnetic moment*, *Eur. Phys. J. C* **74** (2014) 3008, [arXiv:1401.0832].
- [16] F. Jegerlehner, *The Anomalous Magnetic Moment of the Muon, Second Edition*, *Springer Tracts Mod. Phys.* **274** (2017) pp.1–693.
- [17] A. E. Dorokhov, A. P. Martynenko, F. A. Martynenko, A. E. Radzhabov, and A. S. Zhevlakov, *The LbL contribution to the muon $g-2$ from the axial-vector mesons exchanges within the nonlocal quark model*, *EPJ Web Conf.* **212** (2019) 05001, [arXiv:1910.07815].
- [18] P. Masjuan, P. Roig, and P. Sanchez-Puertas, *The interplay of transverse degrees of freedom and axial-vector mesons with short-distance constraints in $g-2$* , *J. Phys. G* **49** (2022), no. 1 015002, [arXiv:2005.11761].
- [19] A. E. Radzhabov, A. S. Zhevlakov, A. P. Martynenko, and F. A. Martynenko, *Light-by-light contribution to the muon anomalous magnetic moment from the axial-vector mesons exchanges within the nonlocal quark model*, *Phys. Rev. D* **108** (2023), no. 1 014033, [arXiv:2301.12641].
- [20] J. Leutgeb and A. Rebhan, *Axial vector transition form factors in holographic QCD and their contribution to the anomalous magnetic moment of the muon*, *Phys. Rev. D* **101** (2020) 114015, [arXiv:1912.01596].
- [21] L. Cappiello, O. Catà, G. D’Ambrosio, D. Greynat, and A. Iyer, *Axial-vector and pseudoscalar mesons in the hadronic light-by-light contribution to the muon $(g-2)$* , *Phys. Rev. D* **102** (2020) 016009, [arXiv:1912.02779].
- [22] M. Hoferichter and P. Stoffer, *Asymptotic behavior of meson transition form factors*, *JHEP* **05** (2020) 159, [arXiv:2004.06127].
- [23] H. R. Grigoryan and A. V. Radyushkin, *Anomalous Form Factor of the Neutral Pion in Extended AdS/QCD Model with Chern-Simons Term*, *Phys. Rev.* **D77** (2008) 115024, [arXiv:0803.1143].
- [24] J. Leutgeb and A. Rebhan, *Hadronic light-by-light contribution to the muon $g-2$ from holographic QCD with massive pions*, *Phys. Rev. D* **104** (2021), no. 9 094017, [arXiv:2108.12345].
- [25] J. Leutgeb, J. Mager, and A. Rebhan, *Hadronic light-by-light contribution to the muon $g-2$ from holographic QCD with solved $U(1)_A$ problem*, *Phys. Rev. D* **107** (2023), no. 5 054021, [arXiv:2211.16562].
- [26] E. Katz and M. D. Schwartz, *An Eta primer: Solving the $U(1)$ problem with AdS/QCD*, *JHEP* **08** (2007) 077, [arXiv:0705.0534].
- [27] T. Schäfer, *Euclidean correlation functions in a holographic model of QCD*, *Phys. Rev. D* **77** (2008) 126010, [arXiv:0711.0236].
- [28] D. K. Hong and D. Kim, *Pseudo scalar contributions to light-by-light correction of muon $g-2$ in AdS/QCD*, *Phys. Lett. B* **680** (2009) 480–484, [arXiv:0904.4042].
- [29] R. Casero, E. Kiritsis, and A. Paredes, *Chiral symmetry breaking as open string tachyon condensation*, *Nucl. Phys. B* **787** (2007) 98–134, [hep-th/0702155].
- [30] M. Järvinen, E. Kiritsis, F. Nitti, and E. Préau, *Tachyon-dependent Chern-Simons terms and the V-QCD baryon*, *JHEP* **12** (2022) 160, [arXiv:2209.05868].
- [31] M. Zanke, M. Hoferichter, and B. Kubis, *On the transition form factors of the axial-vector resonance*

- $f_1(1285)$ and its decay into e^+e^- , *JHEP* **07** (2021) 106, [arXiv:2103.09829].
- [32] I. Iatrakis, E. Kiritsis, and A. Paredes, *An AdS/QCD model from Sen's tachyon action*, *Phys. Rev. D* **81** (2010) 115004, [arXiv:1003.2377].
- [33] I. Iatrakis, E. Kiritsis, and A. Paredes, *An AdS/QCD model from tachyon condensation: II*, *JHEP* **11** (2010) 123, [arXiv:1010.1364].
- [34] M. Järvinen and E. Kiritsis, *Holographic Models for QCD in the Veneziano Limit*, *JHEP* **03** (2012) 002, [arXiv:1112.1261].
- [35] C. Córdova, D. S. Freed, H. T. Lam, and N. Seiberg, *Anomalies in the Space of Coupling Constants and Their Dynamical Applications I*, *SciPost Phys.* **8** (2020), no. 1 001, [arXiv:1905.09315].
- [36] H. Kanno and S. Sugimoto, *Anomaly and superconnection*, *PTEP* **2022** (2022), no. 1 013B02, [arXiv:2106.01591].
- [37] P. Kraus and F. Larsen, *Boundary string field theory of the D anti-D system*, *Phys. Rev. D* **63** (2001) 106004, [hep-th/0012198].
- [38] T. Takayanagi, S. Terashima, and T. Uesugi, *Brane - anti-brane action from boundary string field theory*, *JHEP* **03** (2001) 019, [hep-th/0012210].
- [39] D. Quillen, *Superconnections and the Chern character*, *Topology* **24** (1985), no. 1 89–95.
- [40] J. Erlich, E. Katz, D. T. Son, and M. A. Stephanov, *QCD and a holographic model of hadrons*, *Phys. Rev. Lett.* **95** (2005) 261602, [hep-ph/0501128].
- [41] L. Da Rold and A. Pomarol, *Chiral symmetry breaking from five-dimensional spaces*, *Nucl. Phys. B* **721** (2005) 79–97, [hep-ph/0501218].
- [42] Z. Abidin and C. E. Carlson, *Strange hadrons and kaon-to-pion transition form factors from holography*, *Phys. Rev. D* **80** (2009) 115010, [arXiv:0908.2452].
- [43] J. Leutgeb, A. Rebhan, and M. Stadlbauer, *Hadronic vacuum polarization contribution to the muon $g-2$ in holographic QCD*, *Phys. Rev. D* **105** (2022), no. 9 094032, [arXiv:2203.16508].
- [44] M. A. Shifman, A. I. Vainshtein, and V. I. Zakharov, *QCD and Resonance Physics. Theoretical Foundations*, *Nucl. Phys. B* **147** (1979) 385–447.
- [45] B. Melic, D. Mueller, and K. Passek-Kumericki, *Next-to-next-to-leading prediction for the photon to pion transition form-factor*, *Phys. Rev. D* **68** (2003) 014013, [hep-ph/0212346].
- [46] F. Hechenberger, J. Leutgeb, and A. Rebhan, *Radiative meson and glueball decays in the Witten-Sakai-Sugimoto model*, *Phys. Rev. D* **107** (2023), no. 11 114020, [arXiv:2302.13379].
- [47] P. Colangelo, F. Giannuzzi, and S. Nicotri, *Hadronic light-by-light scattering contributions to $(g-2)_\mu$ from axial-vector and tensor mesons in the holographic soft-wall model*, *Phys. Rev. D* **109** (2024), no. 9 094036, [arXiv:2402.07579].
- [48] U. Gürsoy and E. Kiritsis, *Exploring improved holographic theories for QCD: Part I*, *JHEP* **02** (2008) 032, [arXiv:0707.1324].
- [49] U. Gürsoy, E. Kiritsis, and F. Nitti, *Exploring improved holographic theories for QCD: Part II*, *JHEP* **02** (2008) 019, [arXiv:0707.1349].
- [50] M. Hoferichter, B.-L. Hoid, B. Kubis, S. Leupold, and S. P. Schneider, *Dispersion relation for hadronic light-by-light scattering: pion pole*, *JHEP* **10** (2018) 141, [arXiv:1808.04823].
- [51] A. Gérardin, H. B. Meyer, and A. Nyffeler, *Lattice calculation of the pion transition form factor with $N_f = 2 + 1$ Wilson quarks*, *Phys. Rev. D* **100** (2019), no. 3 034520, [arXiv:1903.09471].
- [52] J. Lüdtke, M. Procura, and P. Stoffer, *Dispersion relations for the hadronic VVA correlator*, arXiv:2410.11946.
- [53] **L3** Collaboration, P. Achard et al., *$f_1(1285)$ formation in two-photon collisions at LEP*, *Phys. Lett. B* **526** (2002) 269–277, [hep-ex/0110073].
- [54] **L3** Collaboration, P. Achard et al., *Study of resonance formation in the mass region 1400 – 1500 MeV through the reaction $\gamma\gamma \rightarrow K_S^0 K^\pm \pi^\mp$* , *JHEP* **03** (2007) 018.
- [55] **Particle Data Group** Collaboration, S. Navas et al., *Review of particle physics*, *Phys. Rev. D* **110** (2024), no. 3 030001.
- [56] M. Hoferichter, B. Kubis, and M. Zanke, *Axial-vector transition form factors and $e^+e^- \rightarrow f_1 \pi^+ \pi^-$* , *JHEP* **08** (2023) 209, [arXiv:2307.14413].
- [57] **SND** Collaboration, M. N. Achasov et al., *Search for direct production of the $f_1(1285)$ resonance in e^+e^- collisions*, *Phys. Lett. B* **800** (2020) 135074, [arXiv:1906.03838].
- [58] H. Leutwyler, *On the $1/N$ expansion in chiral perturbation theory*, *Nucl. Phys. B Proc. Suppl.* **64** (1998) 223–231, [hep-ph/9709408].
- [59] R. Escribano and J.-M. Frère, *Study of the η - η' system in the two mixing angle scheme*, *JHEP* **06** (2005) 029, [hep-ph/0501072].
- [60] **RQCD** Collaboration, G. S. Bali, V. Braun, S. Collins, A. Schäfer, and J. Simeth, *Masses and decay constants of the η and η' mesons from lattice QCD*, *JHEP* **08** (2021) 137, [arXiv:2106.05398].
- [61] P. Roig and P. Sanchez-Puertas, *Axial-vector exchange contribution to the hadronic light-by-light piece of the muon anomalous magnetic moment*, *Phys. Rev. D* **101** (2020) 074019, [arXiv:1910.02881].
- [62] K.-C. Yang, *Light-cone distribution amplitudes of axial-vector mesons*, *Nucl. Phys. B* **776** (2007) 187–257, [arXiv:0705.0692].
- [63] G. Eichmann, C. S. Fischer, T. Haeuser, and O. Regenfelder, *Axial-vector and scalar contributions to hadronic light-by-light scattering*, arXiv:2411.05652.
- [64] S. Holz, M. Hoferichter, B.-L. Hoid, and B. Kubis, *A precision evaluation of the η - and η' -pole contributions to hadronic light-by-light scattering in the anomalous magnetic moment of the muon*, arXiv:2411.08098.
- [65] P. Colangelo, F. Giannuzzi, and S. Nicotri, *π^0 , η , η' two-photon transition form factors in the holographic soft-wall model and contributions to $(g-2)_\mu$* , *Phys. Lett. B* **840** (2023) 137878, [arXiv:2301.06456].
- [66] J. Mager, L. Cappiello, J. Leutgeb, and A. Rebhan, *Longitudinal short-distance constraints on hadronic light-by-light scattering and tensor meson contributions to the muon $g-2$* , arXiv:2501.19293.
- [67] H. J. Kwee and R. F. Lebed, *Pion form-factors in holographic QCD*, *JHEP* **01** (2008) 027, [arXiv:0708.4054].
- [68] M. Hoferichter, P. Stoffer, and M. Zillinger, *Complete Dispersive Evaluation of the Hadronic Light-by-Light Contribution to Muon $g-2$* , *Phys. Rev. Lett.* **134** (2025), no. 6 061902, [arXiv:2412.00190].
- [69] M. Hoferichter, P. Stoffer, and M. Zillinger, *Dispersion*

- relation for hadronic light-by-light scattering: subleading contributions, *JHEP* **02** (2025) 121, [[arXiv:2412.00178](#)].
- [70] I. Danilkin and M. Vanderhaeghen, *Light-by-light scattering sum rules in light of new data*, *Phys. Rev.* **D95** (2017), no. 1 014019, [[arXiv:1611.04646](#)].
- [71] L. Cappiello, J. Leutgeb, J. Mager, and A. Rebhan, *Tensor meson transition form factors in holographic QCD and the muon $g-2$* , [arXiv:2501.09699](#).
- [72] L. Cappiello, O. Catà, and G. D'Ambrosio, *Scalar resonances in the hadronic light-by-light contribution to the muon ($g-2$)*, *Phys. Rev. D* **105** (2022), no. 5 056020, [[arXiv:2110.05962](#)].
- [73] P. Kroll, *A study of the $\gamma^* - f_0(980)$ transition form factors*, *Eur. Phys. J. C* **77** (2017), no. 2 95, [[arXiv:1610.01020](#)].
- [74] V. Shtabovenko, R. Mertig, and F. Orellana, *FeynCalc 9.3: New features and improvements*, *Comput. Phys. Commun.* **256** (2020) 107478, [[arXiv:2001.04407](#)].
- [75] T. Hahn and M. Perez-Victoria, *Automatized one loop calculations in four-dimensions and D-dimensions*, *Comput. Phys. Commun.* **118** (1999) 153–165, [[hep-ph/9807565](#)].